

# Statistical-QoS Driven Energy-Efficiency Optimization Over Green 5G Mobile Wireless Networks

Wenchi Cheng, *Member, IEEE*, Xi Zhang, *Fellow, IEEE*, and Hailin Zhang, *Member, IEEE*

**Abstract**—Since the Information & Communications Technologies (ICT) were designed without taking the energy-saving into account, the unexpected excessive energy consumption of the fourth-generation (4G) and pre-4G wireless networks causes serious carbon dioxide emissions. To achieve green wireless networks, the fifth-generation (5G) wireless networks are expected to significantly increase the network energy efficiency while guaranteeing the quality-of-service (QoS) for time-sensitive multimedia wireless traffics. In this paper, we develop the statistical delay-bounded QoS driven green power allocation schemes to maximize the *effective power efficiency* (EPE), which is defined as the statistical-QoS-guaranteed throughput (effective capacity) per unit power, over single-input single-output (SISO) and multiple-input multiple-output (MIMO)-channels based 5G mobile wireless networks. For the SISO-channel based 5G wireless networks, our developed QoS-driven green power allocation scheme converges to the despicking water-filling scheme (despicking channel inversion scheme) when the QoS constraint becomes very loose (stringent). This scheme and its analyses can be also extended to the diversity-based MIMO wireless networks, but not to the multiplexing-based MIMO wireless networking systems. To this end, we also further develop and analyze the statistical-QoS-driven green power allocation scheme to maximize the EPE over the multiplexing-MIMO based 5G mobile wireless networks. The obtained numerical results show that our developed statistical QoS-driven green power allocation schemes can optimize the EPE over 5G mobile wireless networks, thus enabling the effective implementation of green 5G wireless networks.

**Index Terms**—Green 5G mobile wireless networks, statistical quality-of-service (QoS), power allocation, effective power efficiency (EPE), average power constraint, peak power constraint, single-input single-output (SISO), multiple-input multiple-output (MIMO).

## I. INTRODUCTION

**T**HE unprecedented expansion of Information & Communications Technologies (ICT) industry has resulted in excessive energy consumption in the fourth-generation (4G) and pre-4G wireless networks. It has been pointed out that

Manuscript received 31 July 2015; revised 5 January 2016 and 15 March 2016. This work of Xi Zhang was supported in part by the U.S. National Science Foundation under Grants ECCS-1408601 and CNS-1205726, and the U.S. Air Force under Contract FA9453-15-C-0423. This work of Wenchi Cheng and Hailin Zhang was supported in part by the National Natural Science Foundation of China (No. 61401330 & No. 61301169), the 111 Project of China (B08038), and the Fundamental Research Funds for the Central Universities (No. 7214603701).

X. Zhang is with the Networking and Information Systems Laboratory, Department of Electrical and Computer Engineering, Texas A&M University, College Station, TX 77843 USA (e-mail: xizhang@ece.tamu.edu) (*Corresponding Author*).

W. Cheng and H. Zhang are with the State Key Laboratory of Integrated Services Networks, Xidian University, Xi'an, 710071, China (e-mail: wcheng@xidian.edu.cn; hlzhang@xidian.edu.cn).

the ICT industry causes 2% to 3% of the world-wide carbon dioxide emissions, which is about one quarter of the carbon dioxide emissions by cars in the world [1], [2]. However, the ICT industry has the significant potential to increase its energy efficiency and power efficiency, thus offering the opportunities to significantly reduce current global carbon dioxide emissions in the next generation wireless networks [3]. Recently, the International Telecommunication Union (ITU) has launched the outlines for the next generation, i.e., the fifth-generation (5G), wireless networks. The 5G wireless networks are expected to be green wireless networks, which yields very low carbon dioxide emissions. In particular, the network energy efficiency or power efficiency is required to be increased to 100-fold in 5G wireless networks as compared with that of 4G wireless networks.

The key of increasing network energy efficiency or power efficiency is to optimize the spectrum efficiency per unit power [4], [5]. To achieve maximum spectrum efficiency for each unit power, we need to take into account all different kinds of power limitations for 5G wireless networks. There are two types of power limitations, which affect the network energy efficiency or power efficiency. One is the average power constraint, which is the power limitation averaged over a period of time, and the other is the peak power constraint, which is the instantaneous maximum power supported by the hardware [6], [7]. For green 5G wireless networks, it is demanded to take both the average power constraint and the peak power constraint into account to achieve the maximum network energy efficiency or power efficiency.

On the other hand, green 5G wireless networks need to not only optimize the network energy efficiency or power efficiency alone, but also guarantee the quality-of-service (QoS) for 5G wireless traffics. By integrating the information theory with the statistical QoS provisioning principle, a great deal of efforts have been made to maximize the effective capacity, which is defined as the maximum constant arrival rate that can be supported by the service rate to guarantee the specified QoS requirement, for 4G wireless networks [8]–[14]. However, these research works only take into account the average power constraint for wireless networks, thus being unable to maximize the energy efficiency or power efficiency of 5G wireless networks.

Jointly considering the energy efficiency and the delay-bounded QoS provisioning problems imposes the energy efficient delay-bounded QoS provisioning problem in 5G wireless networks. There are some existing research works focusing on energy-efficient design and/or delay-bounded QoS provisioning for wireless networks [15]–[22]. The authors of [15] proposed a new design framework of cooperative green het-

erogeneous networks, which aims at balancing and optimizing spectrum efficiency, energy efficiency, and QoS in 5G wireless networks. However, this magazine paper didn't give the specified schemes on how to maximize the energy efficiency under QoS constraints. For device-to-device (D2D) based energy-efficient 5G wireless networks, the authors of [16] proposed an energy efficient power control scheme for resource sharing between cellular and D2D users in cellular networks. For full-duplex based energy-efficient 5G wireless networks, the authors of [17] developed the power control schemes to increase the energy efficiency of full-duplex relay based wireless networks. They showed that there is a tradeoff between energy efficiency and spectrum efficiency in shared full-duplex relay wireless networks. The authors of [18] developed the power allocation schemes to maximize the energy efficiency and derived the generic signal-to-interference-plus-noise ratio to simplify the analyses for energy efficiency of 5G candidate techniques based wireless networks. However, these research works didn't take QoS constraints into account. For delay-bounded QoS provisioning, the authors of [19] proposed the delay-aware cooperative scheme to minimize energy cost in cognitive radio based 5G wireless networks. Taking into account the non-zero circuit power, the authors of [20] showed that the optimal energy efficiency can be achieved by deriving the optimum average input power level and distributing the power optimally over time. The achievable energy efficiency decreases as the Nakagami- $m$  parameter  $m$  increases under loose delay-bounded QoS constraints, while the achievable energy efficiency increases as  $m$  increases under stringent delay-bounded QoS constraints. Considering the buffer-empty case for the transmitter buffer, the authors of [21] built the corresponding effective energy efficiency model and develop the cross-layer resource allocation scheme to jointly optimize the transmit power and delay-bounded QoS. However, they didn't take the peak power constraints into consideration.

In our tutorial paper [22], we proposed the heterogenous statistical delay-bounded quality-of-service (QoS) provisioning-based power allocation schemes to maximize the aggregate effective capacity for the following three powerful network architectures: device-to-device, full-duplex, and cognitive radio communications based 5G wireless networks, respectively. However, this previous work mainly focused on deriving the optimal aggregate effective capacity solely under the heterogenous statistical QoS guarantees without concerning/addressing the energy efficiency or effective power efficiency (EPE) issues which is critical for green 5G wireless networks. In order to meet the high energy-efficiency requests for green 5G wireless networks, in this paper we formally define the new energy efficiency metrics and propose the corresponding new schemes to implement green communications in 5G wireless networks. Instead of deriving the aggregate effective capacity under the heterogenous statistical QoS provision framework [22], this paper will mainly focus on developing the effective power efficiency based QoS-driven green power-allocation schemes over the multiplexing MIMO-channel links for green 5G mobile wireless networks.

To maximize the energy efficiency while guaranteeing QoS for 5G wireless networks, in this paper we propose the statisti-

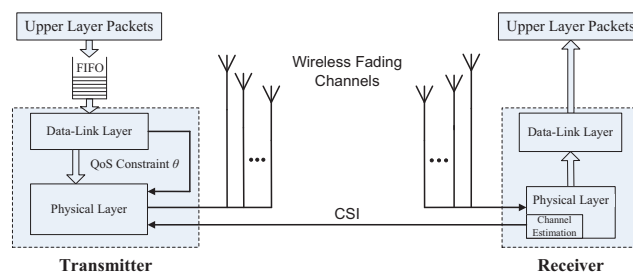


Fig. 1. The point-to-point 5G wireless network system model.

cal delay-bounded QoS-driven green power allocation schemes to maximize the *effective power efficiency* (EPE), which is defined as the *effective capacity per unit power*, under joint average and peak power constraints. First, for SISO-channel based 5G wireless networks, we formulate the EPE maximization problem, which is a strictly convex optimization problem. We derive and analyze the statistical QoS-driven green power allocation schemes under the following three scenarios: (1) the joint average and peak power constraints dominate, (2) only the peak power constraint dominates, and (3) only the average power constraint dominates the QoS-driven power allocation scheme, respectively. Second, for MIMO-channel based 5G wireless networks, because the statistical QoS-driven green power allocation scheme developed for SISO-channel can only be extended to the diversity-based MIMO wireless networks, we further derive and analyze the statistical QoS-driven green power allocation schemes for multiplexing-based MIMO wireless networks. The obtained numerical results show that our proposed QoS-driven green power allocation schemes can maximize EPE of 5G mobile wireless networks, thus enabling the effective implementation of green and QoS-guaranteed 5G mobile wireless networks.

The rest of this paper is organized as follows. Section II describes our 5G wireless network system model and introduces the principle of effective power efficiency, which is characterized under the statistical QoS provisioning. Section III develops the QoS-driven green power allocation scheme to maximize the effective power efficiency of SISO-channel based 5G wireless networks. Section IV develops the QoS-driven green power allocation scheme for the multiplexing MIMO-channel based 5G wireless networks. Section V numerically evaluates our developed QoS-driven green power allocation schemes for the SISO-channel and multiplexing MIMO-channel based 5G wireless networks, respectively. The paper concludes with Section VI.

## II. THE 5G WIRELESS NETWORK SYSTEM MODEL

We consider the point-to-point system, which is shown in Fig. 1, between the transmitter and the receiver in 5G wireless networks. We denote by  $\bar{P}$  and  $P_{\text{peak}}$  the average transmit power constraint and the peak transmit power constraint, respectively. As illustrated in Fig. 1, the upper layer packets are buffered in first-in-first-out (FIFO) queue to be transmitted to their destinations. At the data-link layer, the packets are divided into frames and then split into bit-streams at the

physical layer. The channel power gains follow the stationary block fading model, where they remain unchanged during a time frame with the fixed length  $T_f$ , but vary independently across different time frames. The frame duration  $T_f$  is assumed to be less than the fading coherence time, but sufficiently long so that the information-theoretic assumption of infinite code-block length is meaningful.

We use the Nakagami- $m$  channel model which is very generic and often best fits land-mobile and indoor-mobile multiple propagations. The probability density function (PDF) for the Nakagami- $m$  channel model, denoted by  $p_\Gamma(\gamma)$ , can be expressed as follows:

$$p_\Gamma(\gamma) = \frac{\gamma^{m-1}}{\Gamma(m)} \left(\frac{m}{\bar{\gamma}}\right)^m \exp\left(-\frac{m}{\bar{\gamma}}\gamma\right), \quad \gamma \geq 0, \quad (1)$$

where  $\Gamma(\cdot)$  denotes the Gamma function,  $m$  represents the fading parameter of Nakagami- $m$  distribution,  $\gamma$  denotes the instantaneous channel signal-to-noise ratio (SNR), and  $\bar{\gamma}$  is the average received SNR at the receiver.

#### A. Preliminaries on Statistical Delay-Bounded QoS Provisioning

Based on large deviation principle (LDP), the author of [23] showed that with sufficient conditions, the queue length process  $Q(t)$  converges in distribution to a random variable  $Q(\infty)$  such that

$$-\lim_{Q_{th} \rightarrow \infty} \frac{\log(\Pr\{Q(\infty) > Q_{th}\})}{Q_{th}} = \theta \quad (2)$$

where  $Q_{th}$  is the queue length bound and the parameter  $\theta > 0$  is a real-valued number. The parameter  $\theta$ , which is called the *QoS exponent*, measures the exponential decay rate of the delay-bound QoS violation probabilities. A larger  $\theta$  corresponds to a faster decay rate, which implies that the system can provide a more *stringent* QoS requirement. A smaller  $\theta$  leads to a slower decay rate, which indicates a *looser* QoS requirement. Asymptotically, when  $\theta \rightarrow \infty$ , this implies that the system cannot tolerate any delay, which corresponds to the very stringent statistical delay-bound QoS constraint. On the other hand, when  $\theta \rightarrow 0$ , the system can tolerate an arbitrarily long delay, which corresponds to the very loose statistical delay-bound QoS constraint.

The sequence  $\{R[k], k = 1, 2, \dots\}$  is defined as the data service-rate, which is a discrete-time stationary and ergodic stochastic process. The parameter  $k$  represents the time frame index with a fixed time-duration equal to  $T$ . The  $R[k]$  changes from frame to frame and  $S[t] \triangleq \sum_{k=1}^t R[k]$  represents the partial sum of the service process. The Gartner-Ellis limit of  $S[t]$ , expressed as  $\Lambda_C(\theta) = \lim_{t \rightarrow \infty} (1/t) \log(\mathbb{E}\{e^{\theta S[t]}\})$ , is a convex function differentiable for all real-valued  $\theta$ , where  $\mathbb{E}\{\cdot\}$  denotes the expectation. The effective capacity is defined as the maximum constant arrival rate which can be supported by the service rate to guarantee the specified QoS exponent  $\theta$  [24]. If the service-rate sequence  $R[k]$  is stationary and time-uncorrelated, we can derive the effective capacity as follows [10]:

$$C(\theta) = -\frac{\Lambda_C(-\theta)}{\theta} = -\frac{1}{\theta} \log\left(\mathbb{E}\left\{e^{-\theta R[k]}\right\}\right). \quad (3)$$

#### B. Effective Power Efficiency (EPE) Under Statistical QoS Provisioning

We model the power consumption under statistical QoS provisioning, denoted by  $P_o(\theta)$ , as follows:

$$P_o(\theta) = \alpha \mathbb{E}_\gamma \{P_t(\theta, \gamma)\} + P_c = \alpha \bar{P}_t(\theta) + P_c, \quad (4)$$

where  $\alpha$  is the average-transmit power-consumption coefficient that scales up with the average transmit power due to amplifier loss,  $\mathbb{E}_\gamma$  represents the expectation with respect to instantaneous CSI  $\gamma$ ,  $P_t(\theta, \gamma)$  represents the instantaneous power allocation corresponding to the given  $\gamma$  and QoS exponent  $\theta$ . Intuitively,  $\alpha \in [1, \infty)$  is the reciprocal of the power amplifier efficiency which varies in the range of  $(0, 1]$ . The term  $P_c$  is the circuit power consumption which is independent of the average transmit power.

We define the effective power efficiency (EPE), denoted by  $\mathcal{E}(\theta)$ , as the achieved effective capacity per unit power, which can be formulated as follows:

$$\mathcal{E}(\theta) \triangleq \frac{C(\theta)}{P_o(\theta)}. \quad (5)$$

where  $C(\theta)$  and  $P_o(\theta)$  are specified in Eqs. (3) and (4), respectively. By integrating throughput, QoS exponent, power consumption into  $\mathcal{E}(\theta)$ , in the following we can characterize the achieved throughput per unit power under statistical QoS provisioning for green 5G wireless networks.

#### C. Average and Peak Power Constraints for Green 5G Wireless Networks

To achieve maximum EPE, we need to take into account all different kinds of power limitations for 5G wireless networks. There are two types of power limitations: one of them is the average power constraint and the other is the peak power constraint. Based on these two types of power limitations, we need to consider the following three cases:

- 1) The average power constraint dominates the EPE, where the EPE can be maximized without taking into account the peak power constraint;
- 2) The peak power constraint dominates the EPE, where the EPE can be maximized without taking into account the average power constraint;
- 3) The average and peak power constraints jointly dominate the EPE, where the EPE can be maximized by taking both the average and peak power constraints into account.

Then, we will develop the QoS-driven green power allocation schemes to maximize the EPE for the above three scenarios corresponding to SISO-channel and multiplexing MIMO-channel, respectively, based 5G wireless networks in the followings.

### III. QOS-DRIVEN OPTIMAL GREEN POWER ALLOCATION FOR SISO-CHANNEL BASED 5G WIRELESS NETWORKS

For SISO-channel, the instantaneous service rate of one frame, denoted by  $R_a(\nu)$ , can be expressed as follows:

$$R_a(\nu) = T_f B \log_2(1 + P(\nu)\gamma) \quad (6)$$

where  $\nu \triangleq (\theta, \gamma)$  is defined as the *network state information* (NSI) and  $P(\nu)$  is defined as the power allocation scheme. Then, we can formulate the EPE maximization problem, denoted by **P1**, for the SISO-channel based 5G wireless networks under average and peak power constraints as follows:

$$\mathbf{P1:} \quad \arg \max_{P(\nu)} \left\{ \frac{-\frac{1}{\theta} \log(\mathbb{E}_\gamma [e^{-\theta R_a(\nu)}])}{P_o(\theta)} \right\} \quad (7)$$

subject to the following constraints:

$$\begin{cases} \mathbb{E}_\gamma [P(\nu)] \leq \bar{P}; \\ 0 \leq P(\nu) \leq P_{\text{peak}}, \end{cases} \quad (8)$$

where  $P_o(\theta)$  is defined in Eq. (4). The first and the second equations in Eq. (8) denote that the power allocation scheme is constrained by the average power constraint  $\bar{P}$  and the peak power constraint  $P_{\text{peak}}$ , respectively. Since  $\log(\cdot)$  is a monotonically increasing function, we can simplify problem **P1** to a new problem **P2**, expressed as follows:

$$\begin{aligned} \mathbf{P2:} \quad & \arg \min_{P(\nu)} \left\{ \mathbb{E}_\gamma [e^{-\theta R_a(\nu)}] \right\} \\ & = \arg \min_{P(\nu)} \left\{ \mathbb{E}_\gamma [(1 + P(\nu)\gamma)^{-\beta}] \right\} \end{aligned} \quad (9)$$

subject to the constraints given in Eq. (8), where  $\beta = (\theta T_f B) / \log 2$  is the normalized QoS exponent. Since the objective function of problem **P2** is strictly convex with respect to  $P(\nu)$  and the item  $\mathbb{E}_\gamma [P(\nu)]$  is linear with respect to  $P(\nu)$ , problem **P2** is a strictly convex optimization problem.

#### A. QoS-Driven Optimal Green Power Allocation Scheme for SISO-Channel Under the Average Power Constraint

The peak power constraint is always satisfied if  $P_{\text{peak}} \geq g(\bar{P})$  holds, where  $g(\bar{P})$  is the threshold for SISO-based 5G wireless networks to determine whether the peak power constraint is always satisfied or not. The threshold function of  $g(\bar{P})$  is defined as follows:

$$g(\bar{P}) \triangleq \max_{\gamma} \left\{ \frac{\bar{P}}{\gamma_t^{\frac{1}{\beta+1}} \gamma^{\frac{\beta}{\beta+1}}} - \frac{\bar{P}}{\gamma} \right\}, \quad (10)$$

where  $0 < \beta < \infty$  and  $\gamma_t$  is the average-power-dominated cut-off SNR threshold determined by the following equation:

$$\int_{\gamma_t}^{\infty} \left( \frac{\bar{P}}{\gamma_t^{\frac{1}{\beta+1}} \gamma^{\frac{\beta}{\beta+1}}} - \frac{\bar{P}}{\gamma} \right) p_\Gamma(\gamma) d\gamma = \bar{P}. \quad (11)$$

The following theorem derives the closed-form expression of  $g(\bar{P})$  for the further system modeling and analyses.

*Theorem 1:* Letting  $\sigma = \lim_{\theta \rightarrow \infty} \bar{P} \gamma_t^{-\frac{1}{\beta+1}} - \bar{P}$ , the closed-form expression for the threshold function  $g(\bar{P})$  can be determined by

$$g(\bar{P}) = \max \left\{ \left( \frac{\bar{P}}{\gamma_t} \right), \lim_{\gamma \rightarrow \gamma_t^+} \left( \frac{\sigma}{\gamma} \right) \right\} \quad (12)$$

where  $\gamma_t$  is given by Eq. (11).

*Proof:* The proof is provided in Appendix A. ■

In this case of  $P_{\text{peak}} \geq g(\bar{P})$ , the QoS-driven green power allocation scheme is dominated by the average power constraint. Although the power allocation schemes without QoS provisioning [25] and with QoS provisioning [10], respectively, corresponding to the average power constraint case have been well studied, we explicitly derive the condition when the power allocation schemes are determined by the average power constraint ( $P_{\text{peak}} \geq g(\bar{P})$ ). Therefore, we can derive the following Lemma 1.

*Lemma 1:* If  $P_{\text{peak}} \geq g(\bar{P})$  holds, then the QoS-driven green power scheme, which is the solution to **P2**, is given as follows:

$$P(\nu) = \begin{cases} 0, & \text{if } \gamma < \gamma_t; \\ \frac{\bar{P}}{\gamma_t^{\frac{1}{\beta+1}} \gamma^{\frac{\beta}{\beta+1}}} - \frac{\bar{P}}{\gamma}, & \text{if } \gamma \geq \gamma_t, \end{cases} \quad (13)$$

*Proof:* The proof of Lemma 1 can be obtained by referring to [10, Appendix I], where the authors assume that the condition  $P_{\text{peak}} \geq g(\bar{P})$  always holds. ■

#### B. QoS-Driven Optimal Green Power Allocation Scheme for SISO-Channel Under the Peak Power Constraint

If  $P_{\text{peak}} \leq \bar{P}$  holds, the average power constraint is always satisfied. The QoS-driven green power allocation scheme is dominated by the peak power constraint. Thus, we can derive the following Lemma 2.

*Lemma 2:* If  $P_{\text{peak}} \leq \bar{P}$ , then the QoS-driven green power allocation scheme, which is the solution to **P2**, is given as follows:

$$P(\nu) = P_{\text{peak}}. \quad (14)$$

*Proof:* It is easy to derive this Lemma 2 since using the maximum available instantaneous power will always be optimal if the average power constraint can be removed. ■

Clearly, from Lemma 2 we can observe that if the peak power constraint dominates the EPE, the QoS-driven green power allocation scheme for SISO-channel is  $P_{\text{peak}}$ .

#### C. QoS-Driven Optimal Green Power Allocation Scheme for SISO-Channel Under Both Average and Peak Power Constraints

If the following condition:

$$\bar{P} < P_{\text{peak}} < g(\bar{P}) \quad (15)$$

holds, the QoS-driven green power allocation scheme is determined by joint the average and peak power constraints. Before analyzing the effect of the average and the peak power constraints on the power allocation scheme, we provide two types of thresholds, denoted by  $\theta_w(\bar{P}, P_{\text{peak}})$  and  $\theta_c(\bar{P}, P_{\text{peak}})$ , both corresponding to the average power constraint  $\bar{P}$  and the peak power constraint  $P_{\text{peak}}$ . These two types of thresholds are used to decide whether the power allocation scheme is the very loose delay-QoS constraint (water-filling-like) mode, the very stringent delay-QoS constraint (channel-inversion-like) mode, or the not very loose and not very stringent delay-QoS constraint mode. With the water-filling scheme, the SNR increases as the power increases. With the channel

inversion power allocation scheme, the SNR increases as the power decreases. Thus, the peak power constraint limits the water-filling scheme in the high SNR region and the channel inversion scheme in the low SNR region.

The QoS-driven green power allocation scheme under joint the average and peak power constraints is given by the following Theorem 2.

*Theorem 2:* If  $\bar{P} < P_{\text{peak}} < g(\bar{P})$  holds, then the QoS-driven green power allocation scheme, which is the solution to **P2** defined in Eq. (9), is in the form of <sup>1</sup>

$$P(\nu) = \begin{cases} 0, & \text{if } \gamma < \gamma_0; \\ \frac{\bar{P}}{\gamma_0^{\beta+1} \gamma^{\beta}} - \frac{\bar{P}}{\gamma}, & \text{if } \gamma \geq \gamma_0 \text{ and } \frac{\bar{P}}{\gamma_0^{\beta+1} \gamma^{\beta}} - \frac{\bar{P}}{\gamma} \leq P_{\text{peak}}; \\ P_{\text{peak}}, & \text{if } \gamma \geq \gamma_0 \text{ and } \frac{\bar{P}}{\gamma_0^{\beta+1} \gamma^{\beta}} - \frac{\bar{P}}{\gamma} > P_{\text{peak}}, \end{cases} \quad (16)$$

where  $\gamma_0$  is the cut-off SNR threshold and can be numerically obtained by taking Eq. (16) into the following equation

$$\int_{\gamma_0}^{\infty} P(\nu) p_{\Gamma}(\gamma) d\gamma = \bar{P}. \quad (17)$$

*Proof:* The proof is provided in Appendix B. ■

Then, we delve into two limiting cases corresponding to very loose QoS constraint and very stringent QoS constraint, respectively. These results can be directly obtained from Appendix B.

**Case I(A):** For very loose QoS constraint ( $\theta \rightarrow 0$ ),  $P_{\text{peak}} \geq g(\bar{P})$  reduces to

$$P_{\text{peak}} \geq \frac{\bar{P}}{\gamma_t}. \quad (18)$$

**Case I(B):** For very stringent QoS constraint ( $\theta \rightarrow \infty$ ),  $P_{\text{peak}} \geq g(\bar{P})$  reduces to

$$P_{\text{peak}} \geq \frac{\sigma}{\gamma_t}. \quad (19)$$

Using our developed QoS-driven green power allocation scheme, we can derive the maximum EPE for various QoS-requirement service under joint the average and the peak power constraints, denoted by  $E_a(\theta)$ , as follows:

$$E_a(\theta) = -\frac{1}{\theta [\alpha \bar{P}_t(\theta) + P_c]} \log \left( \int_0^{\gamma_0} p_{\Gamma}(\gamma) d\gamma + \int_{\gamma_0}^{\infty} \left[ \left( \frac{\bar{P}\gamma}{\gamma_0} \right)^{-\frac{\beta}{\beta+1}}, (1 + P_{\text{peak}}\gamma)^{-\beta} \right]^+ p_{\Gamma}(\gamma) d\gamma \right) \quad (20)$$

where  $[a_1, a_2]^+ \triangleq \max\{a_1, a_2\}$ , representing the maximum value between  $a_1$  and  $a_2$ .

<sup>1</sup>In Section V, we call this scheme as SISO-based QoS-driven green power allocation scheme.

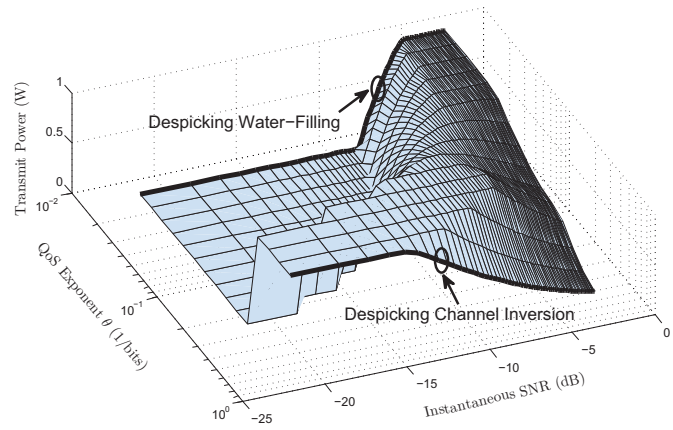


Fig. 2. The optimal power allocation scheme for SISO-channel with  $T_f = 0.2$  ms,  $B = 100$  KHz,  $m = 2$ ,  $\bar{\gamma} = -3$  dB,  $\bar{P} = 0.5$  W and  $P_{\text{peak}} = 1$  W.

To better understand the insights of Theorem 2, we plot the instantaneous power allocation scheme in Fig. 2 using Eqs. (16) and (17). As illustrated in Fig. 2, when the QoS constraint becomes very loose, our developed QoS-driven green power allocation scheme converges to the water-filling-like mode with the peak power constraint despicking in the high SNR region. We name this scheme as *despicking water-filling* (DWF) scheme. When the QoS constraint gets very stringent, our developed QoS-driven green optimal power allocation scheme turns to the channel-inversion-like mode with the peak power constraint despicking in the low SNR region. This scheme is called as *despicking channel inversion* (DCI) scheme. As the QoS exponent  $\theta$  varies between  $(0, \infty)$ , reflecting different delay-QoS constraints, the corresponding power allocation scheme swings between the DWF scheme and the DCI scheme. To thoroughly analyze the effect of joint the average power and the peak power constraints on the power allocation scheme, we discuss two special cases of Theorem 2 - Case II(A) and Case II(B), which yield our QoS-driven green power allocation schemes for the very loose and very stringent QoS constraints, respectively.

**Case II(A):** (Special case for very loose QoS constraint ( $\theta \rightarrow 0$ )). When  $\theta \rightarrow 0$ , our QoS-driven green power allocation scheme derived in Eq. (16) converges to

$$P(\nu) = \begin{cases} 0, & \text{if } \gamma < \gamma_0; \\ \frac{\bar{P}}{\gamma_0} - \frac{\bar{P}}{\gamma}, & \text{if } \gamma_0 \leq \gamma < \gamma^*; \\ P_{\text{peak}}, & \text{if } \gamma^* \leq \gamma, \end{cases} \quad (21)$$

where  $\gamma^* = \bar{P}\gamma_0 / (\bar{P} - P_{\text{peak}}\gamma_0)$  is the despicking SNR threshold of DWF scheme and  $\gamma_0$  can be obtained from Eq. (17). Thus, when the system can tolerate an arbitrarily long delay, our QoS-driven green power allocation scheme reduces to the water-filling algorithm with the peak power constraint despicking in the high SNR region, which is the DWF scheme. In particular, the peak power constraint also affects the cut-off SNR threshold  $\gamma_0$ .

**Case II(B):** (Special case for very stringent QoS constraint ( $\theta \rightarrow \infty$ )). When  $\theta \rightarrow \infty$ , our QoS-driven green power

allocation scheme derived in Eq. (16) converges to

$$P(\nu) = \begin{cases} 0, & \text{if } \gamma < \gamma_0; \\ P_{\text{peak}}, & \text{if } \gamma_0 \leq \gamma < \frac{\omega}{P_{\text{peak}}}; \\ \frac{\omega}{\gamma}, & \text{if } \frac{\omega}{P_{\text{peak}}} \leq \gamma, \end{cases} \quad (22)$$

where  $\omega = \lim_{\theta \rightarrow \infty} \bar{P} \gamma_0^{-\frac{1}{\beta+1}} - \bar{P}$ . Therefore, when the QoS constraint is very stringent, our QoS-driven green power allocation scheme converges to the channel inversion scheme with the peak power despicking in the low SNR region, which is the DCI scheme.

We also derive the EPE by just using the DWF scheme, the DCI scheme, and the constant power allocation scheme to compare with the EPE of our proposed optimal power allocation scheme. Clearly, all of these three ordinary power allocation schemes are independent of the QoS exponent  $\theta$ . If we use the DWF scheme for the system with any QoS exponent  $\theta$ , the EPE, denoted by  $E_w(\theta)$ , can be derived as follows:

$$E_w(\theta) = -\frac{1}{\theta [\alpha \bar{P}_t(\theta) + P_c]} \log \left( \int_0^{\gamma_0} p_{\Gamma}(\gamma) d\gamma + \int_{\gamma_0}^{\frac{\omega}{P_{\text{peak}}}} \left( \frac{\bar{P}\gamma}{\gamma_0} \right)^{-\beta} p_{\Gamma}(\gamma) d\gamma + \int_{\frac{\omega}{P_{\text{peak}}}}^{\infty} (1 + P_{\text{peak}}\gamma)^{-\beta} p_{\Gamma}(\gamma) d\gamma \right). \quad (23)$$

When we apply the DCI scheme for the system with any QoS exponent  $\theta$ , the EPE, denoted by  $E_c(\theta)$ , can be obtained as follows:

$$E_c(\theta) = -\frac{1}{\theta [\alpha \bar{P}_t(\theta) + P_c]} \log \left( \int_0^{\gamma_0} p_{\Gamma}(\gamma) d\gamma + \int_{\gamma_0}^{\frac{\phi}{P_{\text{peak}}}} (1 + P_{\text{peak}}\gamma)^{-\beta} p_{\Gamma}(\gamma) d\gamma + \int_{\frac{\phi}{P_{\text{peak}}}}^{\infty} (1 + \sigma)^{-\beta} p_{\Gamma}(\gamma) d\gamma \right). \quad (24)$$

When the average power constraint is  $\bar{P}$ , to maximize the EPE the constant power allocation scheme need to be  $P(\nu) = \bar{P}$ . Thus, the EPE, denoted by  $E_n(\theta)$ , is derived as

$$E_n(\theta) = -\frac{1}{\theta [\alpha \bar{P}_t(\theta) + P_c]} \cdot \log \left( \int_0^{\infty} (1 + \bar{P}\gamma)^{-\beta} p_{\Gamma}(\gamma) d\gamma \right). \quad (25)$$

In Section V, we will use numerical results to verify the EPE with the QoS-driven green power allocation scheme, the DWF scheme, the DCI scheme, and the constant power allocation scheme specified by Eqs. (20), (23), (24), and (25), respectively.

#### IV. QoS-DRIVEN OPTIMAL GREEN POWER ALLOCATION FOR MULTIPLEXING MIMO-CHANNEL BASED 5G MOBILE WIRELESS NETWORKS

For the diversity-based MIMO system, using diversity combining (for example, maximal-ratio combining), the multichannel transmission problem can be converted into the scalar

channel problem [26], which can be solved by using/extending the QoS-driven green power allocation scheme for SISO-channel that we already developed in Section III.

For the MIMO multiplexing system with  $N_t$  transmit antennas and  $N_r$  receive antennas, the channel matrix  $\mathbf{H}$  can be written using singular value decomposition (SVD) as follows:

$$\mathbf{H} = \mathbf{U} \mathbf{\Lambda} \mathbf{V}^H \quad (26)$$

where  $\mathbf{U}$  and  $\mathbf{V}$  are unitary matrices,  $\mathbf{\Lambda}$  is a diagonal matrix with entries equal to the path gain for the MIMO multiplexing system, and  $H$  denotes the conjugate transpose. Thus, the data streams are equivalent to transmitting through  $N$  parallel singular-value channels, where  $N = \min\{N_t, N_r\}$ . The vector of path gains of  $N$  parallel singular-value channels is denoted by  $\boldsymbol{\lambda} = (\lambda_1, \lambda_2, \dots, \lambda_N)^T$ , where  $\lambda_n$  ( $1 \leq n \leq N$ ) represents the  $n$ -th channel path gain and  $T$  denotes the transpose.<sup>2</sup> Let  $\gamma_n = \lambda_n^2$  ( $1 \leq n \leq N$ ) be the  $n$ -th channel power gain. We define the NSI for MIMO multiplexing systems as  $\tilde{\nu} \triangleq (\theta, \boldsymbol{\lambda})$  and denote by  $P_n(\tilde{\nu})$  ( $1 \leq n \leq N$ ) the power allocation strategy for the  $n$ -th channel.

The instantaneous rate for MIMO multiplexing systems, denoted by  $R_m(\tilde{\nu})$ , is given by

$$\begin{aligned} R_m(\tilde{\nu}) &= T_f B \sum_{n=1}^N \log(1 + P_n(\tilde{\nu})\gamma_n) \\ &= T_f B \sum_{n=1}^N \log(1 + P_n(\tilde{\nu})\lambda_n^2). \end{aligned} \quad (27)$$

Then, we can formulate the optimization problem, denoted by **P3**, for MIMO multiplexing systems as follows:

$$\begin{aligned} \mathbf{P3}: \quad & \arg \max_{P(\tilde{\nu})} \left\{ \frac{-\frac{1}{\theta} \log(\mathbb{E}_{\boldsymbol{\lambda}}[e^{-\theta R_m(\tilde{\nu})}])}{\mathcal{E}(\theta)} \right\} \\ &= \arg \min_{P(\tilde{\nu})} \left\{ \underbrace{\mathbb{E}_{\lambda_1} \cdots \mathbb{E}_{\lambda_N}}_{N\text{-fold}} \left[ \prod_{n=1}^N [1 + P_n(\tilde{\nu})\lambda_n^2]^{-\beta} \right] \right\} \end{aligned} \quad (28)$$

subject to the following constraints:

$$\begin{cases} \sum_{n=1}^N \left\{ \underbrace{\mathbb{E}_{\lambda_1} \cdots \mathbb{E}_{\lambda_N}}_{N\text{-fold}} [P_n(\tilde{\nu})] \right\} \leq \bar{P}; \\ 0 \leq \sum_{n=1}^N P_n(\tilde{\nu}) \leq P_{\text{peak}}, 1 \leq n \leq N. \end{cases} \quad (29)$$

The objective function in Eq. (28) is strictly convex on the space spanned by  $(P_1(\tilde{\nu}), P_2(\tilde{\nu}), \dots, P_n(\tilde{\nu}))$ , which is proved in Appendix I in [11]. In addition, the items  $[\mathbb{E}_{\lambda_1} \cdots \mathbb{E}_{\lambda_N}(P_n(\tilde{\nu}))]$  and  $\sum_{n=1}^N P_n(\tilde{\nu})$  in Eq. (29) are both linear with respect to  $(P_1(\tilde{\nu}), P_2(\tilde{\nu}), \dots, P_n(\tilde{\nu}))$ . Therefore, problem **P3** is a strictly convex optimization problem which can be efficiently solved using the optimization technique.

<sup>2</sup>The PDF for  $\lambda_n$  has the form of  $f(\lambda_n) = \frac{2m^m \lambda_n^{2m-1}}{\Gamma(m)\gamma^m} e^{-\frac{m\lambda_n^2}{\gamma}}$ , which can be derived from Eq. (1).

**A. QoS-Driven Optimal Green Power Allocation Scheme for Multiplexing-Based MIMO Under the Average Power Constraint**

Similar to the analysis for the SISO-channel based 5G wireless networks, we define a threshold  $\tilde{g}(\bar{P})$  to evaluate whether the peak power constraint is always satisfied or not for the multiplexing-based MIMO system. If  $P_{\text{peak}} \geq \tilde{g}(\bar{P})$  holds, the peak power constraint can be removed. Thus, the QoS-driven green power allocation is dominated by the average power constraint. We formulate the Lagrangian function corresponding to problem **P3** for this case as follows:

$$J_a = \underbrace{\mathbb{E}_{\lambda_1} \cdots \mathbb{E}_{\lambda_N}}_{N\text{-fold}} \left\{ \prod_{n=1}^N [1 + P_n(\tilde{\nu}) \lambda_n^2]^{-\beta} \right\} + \tilde{\kappa}_0 \left\{ \sum_{n=1}^N \left[ \underbrace{\mathbb{E}_{\lambda_1} \cdots \mathbb{E}_{\lambda_N}}_{N\text{-fold}} [P_n(\tilde{\nu})] \right] - \bar{P} \right\} \quad (30)$$

where  $\tilde{\kappa}_0$  is the Lagrangian multiplier. Differentiating the Lagrangian function and setting the derivative equal to zero, we obtain a set of  $N$  equations:

$$\frac{\partial J_a}{\partial P_n(\tilde{\nu})} = -\beta \lambda_n^2 [1 + P_n(\tilde{\nu}) \lambda_n^2]^{-\beta-1} f(\lambda) \cdot \prod_{i \in N, i \neq n} [1 + P_i(\tilde{\nu}) \lambda_i^2]^{-\beta} + \tilde{\kappa}_0 f(\lambda) = 0, \quad 1 \leq n \leq N. \quad (31)$$

We define the sets:  $\mathcal{N}_1 \triangleq \{n | P_n(\tilde{\nu}) > 0\}$  and  $\mathcal{N}_0 = \{n | P_n(\tilde{\nu}) \leq 0\}$  with cardinalities  $N_1$  and  $N_0$ , respectively. Then, solving Eq. (31), we can derive the QoS-driven green power allocation scheme for multiplexing-MIMO based 5G mobile wireless networks under the average power constraint as follows [11]:

$$P_n(\tilde{\nu}) = \begin{cases} \frac{\bar{P}}{(\tilde{\lambda}_a)^{\frac{1}{1+N_1\beta}} \prod_{i \in \mathcal{N}_1} \lambda_i^{\frac{2\beta}{1+N_1\beta}}} - \frac{\bar{P}}{\lambda_n^2}, & \text{if } n \in \mathcal{N}_1; \\ 0, & \text{if } n \in \mathcal{N}_0, \end{cases} \quad (32)$$

where  $\tilde{\lambda}_a = \tilde{\kappa}_0/\beta$  is the cut-off SNR threshold and can be numerically obtained by taking Eq. (32) into

$$\sum_{n=1}^N \left[ \underbrace{\mathbb{E}_{\lambda_1} \cdots \mathbb{E}_{\lambda_N}}_{N\text{-fold}} [P_n(\tilde{\nu})] \right] = \bar{P}. \quad (33)$$

Similar to the analysis for the SISO-channel based 5G wireless networks, for the multiplexing-MIMO based 5G mobile wireless networks, we define another threshold function  $\tilde{g}(\bar{P})$  as follows:

$$\tilde{g}(\bar{P}) \triangleq \max_{\lambda_n} \left\{ \sum_{n=1}^{N_1} \left( \frac{\bar{P}}{(\tilde{\lambda}_a)^{\frac{1}{1+N_1\beta}} \prod_{i \in \mathcal{N}_1} \lambda_i^{\frac{2\beta}{1+N_1\beta}}} - \frac{\bar{P}}{\lambda_n^2} \right) \right\} \quad (34)$$

to determine whether the peak power constraint is always satisfied or not. If  $P_{\text{peak}} \geq \tilde{g}(\bar{P})$  holds, the peak power constraint can be removed from part 2 of Eq. (29).

**B. QoS-Driven Optimal Green Power Allocation Scheme for Multiplexing-MIMO Based 5G Networks Under the Peak Power Constraint**

For multiplexing-based MIMO systems, if  $P_{\text{peak}} \leq \bar{P}$  holds, the power allocation scheme is dominated by the peak power constraint. To derive the QoS-driven green power allocation scheme, we can formulate the Lagrangian function corresponding to problem **P3** for this case as follows:

$$J_p = \underbrace{\mathbb{E}_{\lambda_1} \cdots \mathbb{E}_{\lambda_N}}_{N\text{-fold}} \left\{ \prod_{n=1}^N [1 + P_n(\tilde{\nu}) \lambda_n^2]^{-\beta} \right\} + \tilde{\mu} \left( \sum_{n=1}^N P_n(\tilde{\nu}) - P_{\text{peak}} \right) \quad (35)$$

where  $\tilde{\mu}$  is the Lagrangian multiplier. Differentiating the Lagrangian function given by Eq. (35) with respect to  $P_n(\tilde{\nu})$  and setting the derivative equal to zero, we can get

$$\frac{\partial J_p}{\partial P_n(\tilde{\nu})} = -\beta \lambda_n^2 [1 + P_n(\tilde{\nu}) \lambda_n^2]^{-\beta-1} f(\lambda) \cdot \prod_{i \in N, i \neq n} [1 + P_i(\tilde{\nu}) \lambda_i^2]^{-\beta} + \tilde{\mu} = 0, \quad 1 \leq n \leq N. \quad (36)$$

We define the set  $\mathcal{N}_2 = \{n | P_n(\tilde{\nu}) > 0\}$  which can be obtained in the way similar to that of obtaining  $\mathcal{N}_1$ . The cardinality of  $\mathcal{N}_2$  is denoted by  $N_2$ . Then, the optimal green power allocation for the multiplexing-MIMO based 5G mobile wireless networks dominated by the peak power constraint is given by

$$P_n(\tilde{\nu}) = \begin{cases} \frac{\bar{P}}{(\tilde{\gamma}_p)^{\frac{1}{N_2\beta+1}} \prod_{i \in \mathcal{N}_2} \lambda_i^{\frac{2\beta}{N_2\beta+1}}} - \frac{\bar{P}}{\lambda_n^2}, & \text{if } n \in \mathcal{N}_2; \\ 0, & \text{otherwise,} \end{cases} \quad (37)$$

where  $\tilde{\gamma}_p = \tilde{\mu}/[\beta f(\lambda)]$  is the antenna cut-off SNR threshold and can be numerically obtained by taking Eq. (37) into

$$\sum_{n=1}^N P_n(\tilde{\nu}) = P_{\text{peak}}. \quad (38)$$

Equation (37) shows that the optimal power allocated to the  $n$ -th antenna  $P_n(\tilde{\nu})$  is associated with all channel path gains  $\lambda_i$  ( $1 \leq i \leq N$ ). In particular, when  $\theta \rightarrow 0$ , Eq. (37) reduces to

$$P_n(\tilde{\nu}) = \begin{cases} \frac{\bar{P}}{\tilde{\gamma}_p} - \frac{\bar{P}}{\lambda_n^2}, & \text{if } n \in \mathcal{N}_2; \\ 0, & \text{otherwise,} \end{cases} \quad (39)$$

which shows that when the system can tolerate any long delay the optimal power allocation is the water-filling over antennas, but not across time. When  $\theta \rightarrow \infty$ , Eq. (37) turns to

$$P_n(\tilde{\nu}) = \begin{cases} \frac{\bar{P}}{\prod_{i \in \mathcal{N}_2} \lambda_i^{\frac{2}{N_2}}} - \frac{\bar{P}}{\lambda_n^2}, & \text{if } n \in \mathcal{N}_2; \\ 0, & \text{otherwise.} \end{cases} \quad (40)$$

Given that  $\lambda_i^2$  is the power gain of the  $i$ -th singular-value channel, Eq. (40) shows that when the QoS constraint is very stringent the optimal power allocated to  $n$ -th antenna  $P_n(\tilde{\nu})$

$$P_n(\tilde{\nu}) = \begin{cases} \frac{\bar{P}}{\lambda_0^{\frac{1}{1+N_1\beta}} \prod_{i \in \mathcal{N}_1} \lambda_i^{\frac{2\beta}{1+N_1\beta}}} - \frac{\bar{P}}{\lambda_n^2}, & \text{if } n \in \mathcal{N}_1 \text{ and } \sum_{n=1}^N \frac{\bar{P}}{\lambda_0^{\frac{1}{1+N_1\beta}} \prod_{i \in \mathcal{N}_1} \lambda_i^{\frac{2\beta}{1+N_1\beta}}} - \frac{\bar{P}}{\lambda_n^2} < P_{\text{peak}}; \\ \frac{\bar{P}}{(\lambda_0 + \mu_0)^{\frac{1}{1+N_1\beta}} \prod_{i \in \mathcal{N}_1} \lambda_i^{\frac{2\beta}{1+N_1\beta}}} - \frac{\bar{P}}{\lambda_n^2}, & \text{if } n \in \mathcal{N}_1 \text{ and } \sum_{n=1}^N \frac{\bar{P}}{\lambda_0^{\frac{1}{1+N_1\beta}} \prod_{i \in \mathcal{N}_1} \lambda_i^{\frac{2\beta}{1+N_1\beta}}} - \frac{\bar{P}}{\lambda_n^2} \geq P_{\text{peak}}; \\ 0, & \text{otherwise} \end{cases} \quad (42)$$

corresponds to the geometric mean of singular-value channel power gains and the power gain of the  $n$ -th singular-value channel.

### C. QoS-Driven Optimal Green Power Allocation Scheme for Multiplexing-MIMO Based 5G Networks Under Both Average and Peak Power Constraints

If the following condition:

$$\bar{P} < P_{\text{peak}} < \tilde{g}(\bar{P}) \quad (41)$$

holds, the multiplexing-MIMO based 5G networks are affected by the joint average and peak power constraints. The closed-form expression of  $\tilde{g}(\bar{P})$  will be derived in Section IV-A. To maximize the EPE for the multiplexing-MIMO based 5G networks under joint the average and peak power constraints, the optimal power allocation for the multiplexing-MIMO based 5G networks is summarized by Theorem 3 that follows.

**Theorem 3:** If  $\bar{P} < P_{\text{peak}} < \tilde{g}(\bar{P})$  holds, then the joint QoS-driven optimal green power allocation scheme, which is the solution to problem **P3** defined in Eq. (28), is in the form given by Eq. (42),<sup>3</sup> where we define  $\lambda_0 = \kappa_0/\beta$  and  $\mu_0 = \mu/(\beta f(\boldsymbol{\lambda}))$  as the cut-off SNR thresholds corresponding to the average power constraint and peak power constraint, respectively, and  $f(\boldsymbol{\lambda})$  is the PDF of  $\boldsymbol{\lambda}$ . Both  $\lambda_0$  and  $\mu_0$  can be numerically obtained by solving the following equations:

$$\begin{cases} \sum_{n=1}^N \left[ \underbrace{\mathbb{E}_{\lambda_1} \cdots \mathbb{E}_{\lambda_N}}_{N\text{-fold}} (P_n(\tilde{\nu})) \right] = \bar{P}; \\ \sum_{n=1}^N \left( \frac{\bar{P}}{(\lambda_0 + \mu_0)^{\frac{1}{1+N_1\beta}} \prod_{i \in \mathcal{N}_1} \lambda_i^{\frac{2\beta}{1+N_1\beta}}} - \frac{\bar{P}}{\lambda_n^2} \right) = P_{\text{peak}}. \end{cases} \quad (43)$$

*Proof:* The proof is provided in Appendix C. ■

From Theorem 3, we can observe that when the sum of power assigned to all transmit antennas is equal to  $P_{\text{peak}}$ , the optimal power allocation depends on the joint Nakagami- $m$  PDF  $f(\boldsymbol{\lambda})$ . It is also clear that  $\boldsymbol{\lambda}$  can be considered as the square root of the sum of squares of  $m$  independent Rayleigh or  $(2m)$  independent Gaussian variables [27]. Thus,  $\boldsymbol{\lambda}$  can be specified by  $N \times (2m)$  Gaussian random variables, which form an  $N \times (2m)$  matrix. The column vectors of this  $N \times (2m)$  matrix are denoted by  $\mathbf{y}_z$ , for  $z = 1, 2, \dots, (2m)$ . The correlation matrix of these Gaussian random vectors  $\mathbf{y}_z$ , for  $z = 1, 2, \dots, (2m)$ , is denoted by  $\mathcal{C}$ , whose elements  $\rho_{i,j}$ , for  $i = 1, 2, \dots, N$  and  $j = 1, 2, \dots, N$ , are the power

correlations between the  $i$ -th element and the  $j$ -th element of  $N$ -dimensional random vector  $\mathbf{y}_z$ , taking the following values  $\rho_{i,j} = 1$  for  $i = j$  and  $0 < \rho_{i,j} < 1$  for  $i \neq j$ . When the channels between all transmit and receive antenna pairs follow the correlated Nakagami- $m$  distribution, if the inverse of the correlation matrix  $\mathcal{C}$ , denoted by  $\mathcal{C}^{-1}$ , is tridiagonal, then we can derive the joint Nakagami- $m$  PDF of  $\boldsymbol{\lambda}$  as follows [28]:

$$f(\boldsymbol{\lambda}) = \frac{|\mathcal{C}^{-1}|^m \lambda_1^{m-1} \lambda_N^m e^{-\frac{q_{N,N} \lambda_N^2}{2}}}{2^{m-1} \Gamma(m)} \prod_{k=1}^{N-1} \left[ |q_{k,k+1}|^{-(m-1)} \cdot \lambda_k e^{-\frac{q_{k,k} \lambda_k^2}{2}} I_{m-1}(|q_{k,k+1}| \lambda_k \lambda_{k+1}) \right] \quad (44)$$

where  $q_{i,j}$  ( $i = 1, 2, \dots, N$ ;  $j = 1, 2, \dots, N$ ) is the element of matrix  $\mathcal{C}^{-1}$  at the  $i$ -th row and the  $j$ -th column. The function  $I_\varphi(\cdot)$  is the first kind of  $\varphi$ -th order modified Bessel function, which can be expressed as

$$I_{m-1}(b) = \lim_{n \rightarrow \infty} \frac{\sum_{i=0}^n \binom{n}{i} \frac{b^{2i+m-1}}{i! \Gamma(m+i)}, \quad (45)$$

where  $\Gamma(\cdot)$  is the Gamma function. If the matrix  $\mathcal{C}^{-1}$  is not tridiagonal, we can use another matrix  $\tilde{\mathcal{C}}$ , whose inverse is tridiagonal, to approximate the matrix  $\mathcal{C}$ . For example, we can use the Green's matrix approximation [29].

Next, we need to derive the closed-form expression of  $\tilde{g}(\bar{P})$ . Note that if  $P_{\text{peak}} \geq \tilde{g}(\bar{P})$ , we always have

$$\sum_{n=1}^{N_1} \left( \frac{\bar{P}}{(\tilde{\lambda}_a)^{\frac{1}{1+N_1\beta}} \prod_{i \in \mathcal{N}_1} \lambda_i^{\frac{2\beta}{1+N_1\beta}}} - \frac{\bar{P}}{\lambda_n^2} \right) \leq P_{\text{peak}}, \quad (46)$$

where  $\forall \lambda_n \in R^+ \triangleq [0, +\infty)$ . It is very difficult to derive the exactly closed-form expression of  $\tilde{g}(\bar{P})$  based on Eq. (46). However, we can derive a tight upper-bound for  $\tilde{g}(\bar{P})$ . We denote by  $U(\bar{P})$  this tight upper-bound and we have

$$\begin{aligned} & \sum_{n=1}^{N_1} \left( \frac{\bar{P}}{(\tilde{\lambda}_a)^{\frac{1}{1+N_1\beta}} \prod_{i \in \mathcal{N}_1} \lambda_i^{\frac{2\beta}{1+N_1\beta}}} - \frac{\bar{P}}{\lambda_n^2} \right) \\ &= \frac{N_1 \bar{P}}{(\tilde{\lambda}_a)^{\frac{1}{1+N_1\beta}} \prod_{i \in \mathcal{N}_1} \lambda_i^{\frac{2\beta}{1+N_1\beta}}} - \sum_{n=1}^{N_1} \left( \frac{\bar{P}}{\lambda_n^2} \right) \\ &\stackrel{(a)}{\leq} \frac{N_1 \bar{P}}{(\tilde{\lambda}_a)^{\frac{1}{1+N_1\beta}} \prod_{i \in \mathcal{N}_1} \lambda_i^{\frac{2\beta}{1+N_1\beta}}} \\ &\stackrel{(b)}{\leq} \frac{N_1 \bar{P}}{(\tilde{\lambda}_a)^{\frac{1}{1+N_1\beta}} \lambda_{\min}^{\frac{2\beta N_1}{1+N_1\beta}}} = U(\bar{P}), \end{aligned} \quad (47)$$

<sup>3</sup>In Section V, we call this scheme as QoS-driven optimal green power allocation scheme.

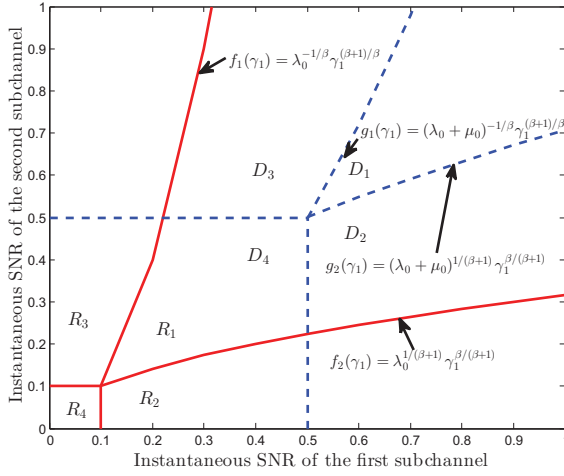


Fig. 3. The scheme regions with  $\gamma_0 = 0.1$ ,  $\mu_0 = 0.4$ , and  $\beta = 1$  when  $N = 2$ .

where  $\lambda_{\min}$  denotes the minimum one among  $\lambda_i$  ( $1 \leq i \leq N_1$ ). Because  $\lambda_n$  ( $1 \leq i \leq N_1$ ) can be any positive real-valued number, (a) in Eq. (47) holds. Due to  $\lambda_{\min} \leq \lambda_i$  ( $1 \leq i \leq N_1$ ), (b) in Eq. (47) holds.

It is surprising to observe that  $U(\bar{P})$  has the similar mathematical structure as  $f_a(\gamma)$ , which is analyzed in Appendix B. Thus, in a similar way as deriving the closed-form expression of  $g(\bar{P})$  (see Eq. (10)), we can obtain  $U(\bar{P})$  as follows:

$$U(\bar{P}) = \max \left\{ \frac{N_1 \bar{P}}{\tilde{\lambda}_a}, \lim_{\lambda_{\min} \rightarrow \sqrt{\tilde{\lambda}_a}} \frac{\tilde{\sigma}}{\lambda_{\min}^2} \right\}, \quad (48)$$

where

$$\tilde{\sigma} = \lim_{\theta \rightarrow \infty} N_1 \bar{P} \left[ \left( \tilde{\lambda}_a \right)^{-\frac{1}{N_1 \beta + 1}} - 1 \right]. \quad (49)$$

Although  $U(\bar{P})$  is the upper-bound of  $\tilde{g}(\bar{P})$ , we can still use our proposed QoS-driven power allocation schemes for MIMO-channel based wireless networks. If  $P_{\text{peak}} \leq \bar{P}$ , we use the power allocation scheme proposed by Eqs. (37) and (38) given in Section IV-B. If  $P_{\text{peak}} \geq U(\bar{P})$ , we employ the power allocation scheme developed by Eqs. (32) and (33) given in Section IV-A. If  $\bar{P} < P_{\text{peak}} < U(\bar{P})$ , we apply the power allocation scheme specified by Eqs. (42) and (43) given in Section IV-C. When  $P_{\text{peak}}$  falls into the region  $[\tilde{g}(\bar{P}), U(\bar{P})]$ , the power allocation scheme specified by Eqs. (42) and (43) can obtain the same solution as the power allocation scheme specified by Eqs. (32) and (33). Thus,  $U(\bar{P})$  can be considered as the condition for which the average power constraint dominates the QoS-driven green power allocation scheme without the peak power constraint imposed.

#### D. The Case of Two Antennas

To demonstrate the execution procedure of our developed QoS-driven optimal green power allocation scheme for multiplexing-MIMO based 5G mobile wireless networks, we consider a particular case when the number of subchannels

$N = 2$ . As shown in Fig. 3, the solid/dash lines partition the SNR-plane spanned by  $(\gamma_1, \gamma_2)$  into four regions, where  $\gamma_1$  and  $\gamma_2$  are the instantaneous SNRs of the first and the second subchannels, respectively. If  $(\gamma_1, \gamma_2)$  falls into the region  $R_1$  ( $D_1$ ), both the first and the second subchannels will be assigned with power for data transmission. If  $(\gamma_1, \gamma_2)$  belongs to the region  $R_2$  ( $D_2$ ) or the region  $R_3$  ( $D_3$ ), only the first subchannel or the second subchannel will be assigned with power. When  $(\gamma_1, \gamma_2)$  falls into region  $R_4$  ( $D_4$ ), the system is in outage state and no power will be assigned. To obtain the boundaries of the region  $R_1$  and the region  $D_1$ , we can formulate the equation as follows:

$$\frac{\bar{P}}{(\lambda_0 + x)^{\frac{1}{1+2\beta}} (\gamma_1 \gamma_2)^{\frac{\beta}{1+2\beta}}} - \frac{\bar{P}}{\gamma_j} = 0, \quad (50)$$

where  $x \in \{0, \mu_0\}$  and  $j \in \{1, 2\}$ . Thus, the boundaries are given by

$$\begin{cases} f_1(\gamma_1) = \lambda_0^{-1/\beta} \gamma_1^{(\beta+1)/\beta}; \\ f_2(\gamma_1) = \lambda_0^{1/(\beta+1)} \gamma_1^{\beta/(\beta+1)}; \\ g_1(\gamma_1) = (\lambda_0 + \mu_0)^{-1/\beta} \gamma_1^{(\beta+1)/\beta}; \\ g_2(\gamma_1) = (\lambda_0 + \mu_0)^{1/(\beta+1)} \gamma_1^{\beta/(\beta+1)}. \end{cases} \quad (51)$$

Once obtained these boundaries, we give the steps or algorithm on how to determine the QoS-driven green power allocation for  $N = 2$  multiplexing-MIMO based 5G mobile wireless networks based on Fig. 3 as follows:

**Step 1:** Calculate the power allocation using the following strategies:

- 1) If  $(\gamma_1, \gamma_2) \in R_1$ :  $P_1(\tilde{\nu}) = \frac{\bar{P}}{\lambda_0^{\frac{1}{1+2\beta}} (\gamma_1 \gamma_2)^{\frac{\beta}{1+2\beta}}} - \frac{\bar{P}}{\gamma_1}$  and  $P_2(\tilde{\nu}) = \frac{\bar{P}}{\lambda_0^{\frac{1}{1+2\beta}} (\gamma_1 \gamma_2)^{\frac{\beta}{1+2\beta}}} - \frac{\bar{P}}{\gamma_2}$ ;
- 2) If  $(\gamma_1, \gamma_2) \in R_2$ :  $P_1(\tilde{\nu}) = \frac{\bar{P}}{\lambda_0^{\frac{1}{1+2\beta}} (\gamma_1 \gamma_2)^{\frac{\beta}{1+2\beta}}} - \frac{\bar{P}}{\gamma_1}$  and  $P_2(\tilde{\nu}) = 0$ ;
- 3) If  $(\gamma_1, \gamma_2) \in R_3$ :  $P_1(\tilde{\nu}) = 0$  and  $P_2(\tilde{\nu}) = \frac{\bar{P}}{\lambda_0^{\frac{1}{1+2\beta}} (\gamma_1 \gamma_2)^{\frac{\beta}{1+2\beta}}} - \frac{\bar{P}}{\gamma_2}$ ;
- 4) If  $(\gamma_1, \gamma_2) \in R_4$ :  $P_1(\tilde{\nu}) = 0$  and  $P_2(\tilde{\nu}) = 0$ .

**Step 2:** Calculate  $P_{\text{sum}}(\tilde{\nu}) = P_1(\tilde{\nu}) + P_2(\tilde{\nu})$ , which is the sum power allocated to the two subchannels. If  $P_{\text{sum}}(\tilde{\nu}) < P_{\text{peak}}$ , go to **Step 4**, else if  $P_{\text{sum}}(\tilde{\nu}) \geq P_{\text{peak}}$ , go to **Step 3**. **Step 3:** Calculate the power allocation using the following strategies:

- 1) If  $(\gamma_1, \gamma_2) \in D_1$ :  $P_1(\tilde{\nu}) = \frac{\bar{P}}{(\lambda_0 + \mu_0)^{\frac{1}{1+2\beta}} (\gamma_1 \gamma_2)^{\frac{\beta}{1+2\beta}}} - \frac{\bar{P}}{\gamma_1}$  and  $P_2(\tilde{\nu}) = \frac{\bar{P}}{(\lambda_0 + \mu_0)^{\frac{1}{1+2\beta}} (\gamma_1 \gamma_2)^{\frac{\beta}{1+2\beta}}} - \frac{\bar{P}}{\gamma_2}$ ;
- 2) If  $(\gamma_1, \gamma_2) \in D_2$ :  $P_1(\tilde{\nu}) = \frac{\bar{P}}{(\lambda_0 + \mu_0)^{\frac{1}{1+2\beta}} (\gamma_1 \gamma_2)^{\frac{\beta}{1+2\beta}}} - \frac{\bar{P}}{\gamma_1}$  and  $P_2(\tilde{\nu}) = 0$ ;

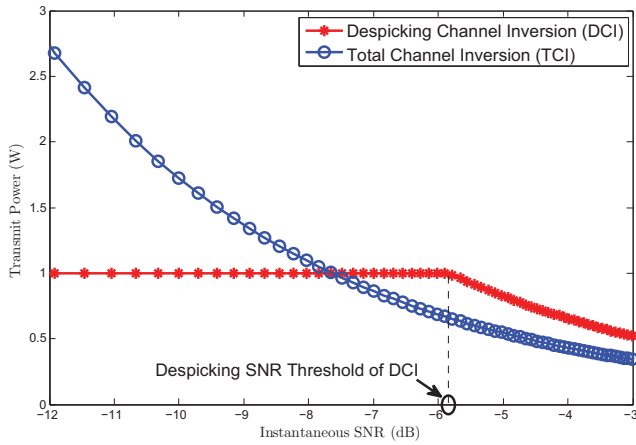


Fig. 4. The transmit power comparison between the DCI scheme and the TCI scheme with  $T_f = 0.2$  ms,  $B = 100$  KHz,  $m = 2$ ,  $\bar{\gamma} = -3$  dB,  $\bar{P} = 0.5$  W, and  $P_{\text{peak}} = 1$  W when  $\theta \rightarrow \infty$ .

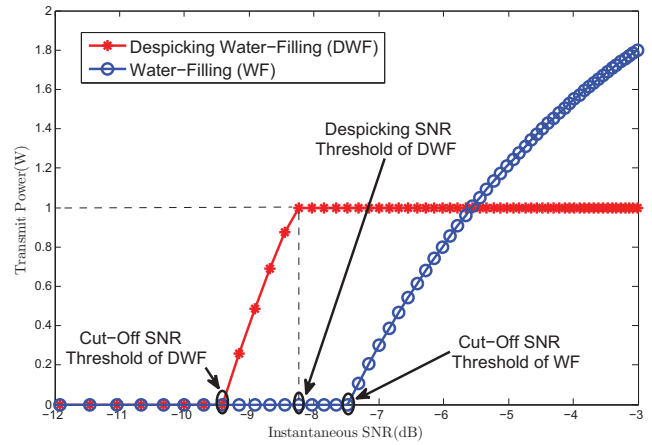


Fig. 5. The transmit power comparison between the DWF scheme and the WF scheme with  $T_f = 0.2$  ms,  $B = 100$  KHz,  $m = 2$ ,  $\bar{\gamma} = -3$  dB,  $\bar{P} = 0.5$  W, and  $P_{\text{peak}} = 1$  W when  $\theta \rightarrow 0$ .

- 3) If  $(\gamma_1, \gamma_2) \in D_3$ :  $P_1(\tilde{\nu}) = 0$  and  $P_2(\tilde{\nu}) = \frac{\bar{P}}{\frac{1}{(\lambda_0 + \mu_0)^{1+2\beta}} (\gamma_1 \gamma_2)^{\frac{\beta}{1+2\beta}} - \frac{\bar{P}}{\gamma_2}}$ ;
- 4) If  $(\gamma_1, \gamma_2) \in D_4$ :  $P_1(\tilde{\nu}) = 0$  and  $P_2(\tilde{\nu}) = 0$ .

**Step 4:** The QoS-drive green power allocation scheme  $(P_1^*(\tilde{\nu}), P_2^*(\tilde{\nu}))$  is given by  $P_1^*(\tilde{\nu}) = P_1(\tilde{\nu})$  and  $P_2^*(\tilde{\nu}) = P_2(\tilde{\nu})$ .

Thus, the maximum EPE for  $N = 2$  multiplexing-based MIMO system, denoted by  $E_2(\tilde{\nu})$ , can be derived as follows:

$$E_2(\tilde{\nu}) = -\frac{1}{\theta [\alpha \bar{P}_t(\theta) + P_c]} \cdot \log \left( \int \prod_{n=1}^2 [1 + P_n^*(\tilde{\nu}) \gamma_n]^{-\beta} f(\lambda) d\gamma_1 d\gamma_2 \right). \quad (52)$$

Due to the complexity of the QoS-driven green power allocation scheme and the joint PDF of Nakagami- $m$  channel, the EPE of multiplexing-MIMO based 5G mobile wireless networks does not have the simple closed-form solution. We use the numerical results to show the EPE of multiplexing-MIMO based 5G mobile wireless networks as compared with the SISO in Section V.

## V. NUMERICAL EVALUATIONS

In this section, we use the numerical analyses to evaluate the performances of our proposed QoS-driven green power allocation schemes. We employ the Nakagami- $m$  channel model with  $\bar{\gamma} = -3$  dB and  $m = 2$ . The EPE is our metric to evaluate the performance of energy-efficient 5G wireless networks. First, since the very loose and stringent delay-bounded QoS requirements are two typical cases, we depict the QoS-driven green power allocation schemes under very loose and very stringent delay-bounded QoS constraints in Figs. 5 and 4, respectively, where our developed QoS-driven green power allocation schemes are the DWF and DCI schemes, respectively. Second, to verify the EPE improvement of our proposed QoS-driven green power allocation schemes over the variations of delay-bounded QoS requirements, Figs. 6 and 7

compare the obtained EPE of our proposed schemes with other related power allocation schemes. To further demonstrate the EPE improvement of our proposed QoS-driven green power allocation schemes, we compare the obtained EPE of our developed schemes with the state-of-the-art schemes [18] in Fig. 8. Third, because the peak power is the newly focused constraints, we compare the EPE of our developed schemes with other related power allocation schemes under peak power constraints in Fig. 10.

We compare our developed QoS-driven power allocation scheme with the despicking water-filling scheme, the despick channel inversion scheme, the constant power allocation scheme, the power allocation scheme given by Lemma 1, and the power allocation scheme developed in reference [18]. The despicking water-filling scheme and the despick channel inversion scheme are both energy-efficient schemes. They are designed for specified delay-bounded QoS constraints. The despicking water-filling scheme and the despick channel inversion scheme can achieve the optimal effective power efficiency for very loose and stringent delay-bounded QoS constraints, respectively. The constant power allocation scheme is simple and easy to be implemented for practical scenarios. The power allocation scheme given by Lemma 1 is a effective-capacity-efficient scheme, which can maximize the effective capacity under average power constraints. The power allocation scheme developed in reference [18] is designed to maximize the effective capacity under both average and peak power constraints.

Figure 5 plots the DWF scheme and the water-filling (WF) scheme when  $\theta \rightarrow 0$ . As shown in Fig. 5, the cut-off SNR threshold of DWF is smaller than the cut-off SNR threshold of WF scheme. This is because for the given average power constraint the saved power due to the power despicking in the high SNR region can be used in the low SNR region. Fig. 4 shows the DCI scheme and the total channel inversion (TCI) scheme when  $\theta \rightarrow \infty$ . As illustrated in Fig. 4, the DCI scheme assigns larger power in the high SNR region than the TCI scheme. This is because for the given average power constraint the saved power due to the power despicking in the low SNR region can be used in the high SNR region.

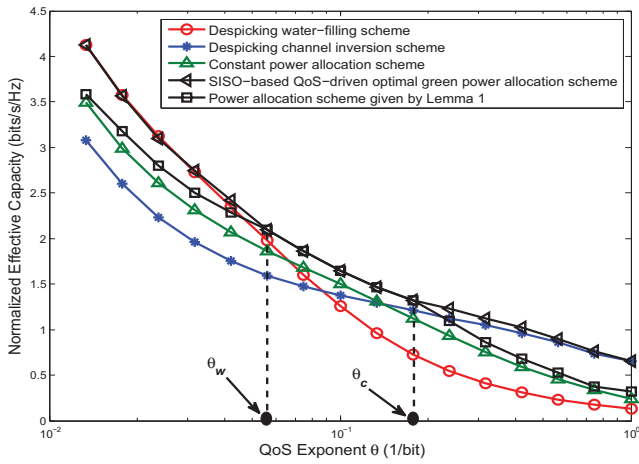


Fig. 6. The EPE of our SISO-based QoS-driven power allocation scheme, the power allocation scheme given by Lemma 1, the despicking water-filling scheme, the despicking channel inversion scheme, and the constant power allocation scheme for the SISO-channel.

To compare our developed QoS-driven green power allocation scheme with the power allocation scheme given by Lemma 1, the DWF scheme, the DCI scheme, and the constant power allocation scheme for the SISO-channel, we plot the normalized EPE of these five schemes in Fig. 6. As illustrated in Fig. 6, our developed QoS-driven green power allocation scheme can achieve larger EPE than the power allocation scheme given by Lemma 1 when the delay-QoS constraint is very loose ( $\theta < \theta_w(\bar{P}, P_{\text{peak}})$ ) or very stringent ( $\theta > \theta_c(\bar{P}, P_{\text{peak}})$ ). This is because the instantaneous allocated power given by Lemma 1 is limited to  $P_{\text{peak}}$  in the high SNR region when the delay-QoS constraint is very loose and in the low region when the delay-QoS constraint is very stringent. When the delay-QoS constraint is not very loose and not very stringent ( $\theta_w(\bar{P}, P_{\text{peak}}) \leq \theta \leq \theta_c(\bar{P}, P_{\text{peak}})$ ), our developed QoS-driven green power allocation scheme can obtain the same EPE as compared with the power allocation scheme given by Lemma 1. This is because the maximum instantaneous allocated power is always less than the peak power constraint  $P_{\text{peak}}$  when the delay-QoS constraint is not very loose and not very stringent. We can also observe that our developed QoS-driven green power allocation scheme can achieve much larger EPE than the DWF scheme, the DCI scheme, and the constant power allocation scheme. When the QoS constraint is very loose, our QoS-driven green power allocation scheme converges to the DWF scheme. When the QoS constraint is very stringent, our QoS-driven green power allocation scheme reduces to the DCI scheme. Our developed QoS-driven green power allocation can achieve the maximum EPE under different delay-QoS constraints.

Figure 7 plots the normalized EPE of our QoS-driven green power allocation scheme, the power allocation scheme only considering average power constraint (see Eq. (32) given in Section IV-A), the DWF scheme, the DCI scheme, and the independent QoS-driven power allocation scheme for the MIMO-channel when considering the joint average and peak power constraints. The independent QoS-driven power allocation

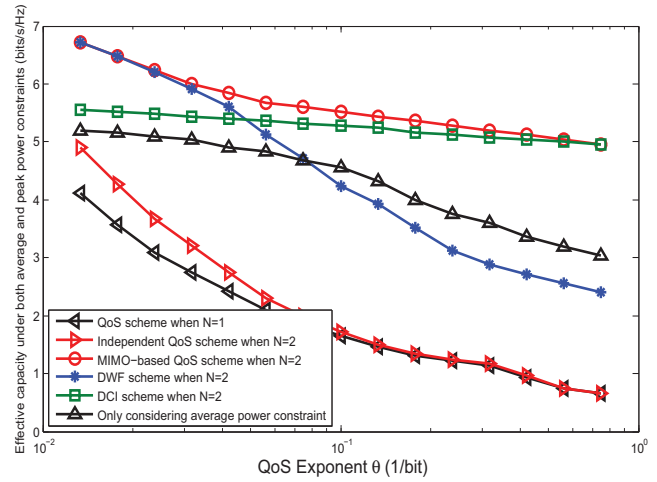


Fig. 7. The EPE of the MIMO-based QoS-driven power allocation scheme, the power allocation scheme only considering average power constraint, the despicking water-filling scheme, the despicking channel inversion scheme, the independent QoS-driven power allocation scheme for the MIMO-channel, and the QoS-driven power allocation scheme for the SISO-channel when considering joint the average and the peak power constraints.

scheme optimizes the first channel and the second channel independently. We also depict the EPE of using the QoS-driven green power allocation scheme for the SISO-channel to compare with the EPE of the MIMO-channel. As shown in Fig. 7, the QoS-driven green power allocation scheme can achieve the largest EPE as compared with the other schemes. The power allocation scheme only considering average power constraint (Eq. (32)) cannot achieve the maximum EPE due to ignoring the peak power constraint. Similar to the SISO-channel, the DWF scheme for the MIMO-channel can obtain the same EPE as the QoS-driven green power allocation scheme when the QoS constraint is very loose. The DCI scheme for the MIMO system can get the same EPE as the QoS-driven green power allocation scheme when the QoS constraint is very stringent. The independent QoS-driven power allocation scheme can achieve larger EPE than the SISO-channel QoS-driven green power allocation scheme when the QoS constraint is very loose, and can even approach the same EPE when the QoS constraint is very stringent. The QoS-driven green power allocation scheme has a big EPE gain as compared with the independent QoS-driven power allocation scheme.

From Figs. 6 and 7, we further observe that our developed QoS-driven green power allocation schemes achieve larger EPE than the other related power allocation schemes. This is because our developed schemes are adaptive to the diverse delay-bounded QoS constraints. Thus, our developed optimal QoS-driven green power allocation schemes can achieve maximum EPE for diverse delay-bounded QoS constraints. Figs. 6 and 7 also show the other two kinds of existing schemes: one is the QoS-driven power allocation schemes taking into account the average power constraints and the other is the power allocation schemes without taking into account the delay-bounded QoS provisioning. For the QoS-driven power allocation schemes which only take into account the average power constraints, the power cannot be efficiently allocated with respect to time because the peak power constraint is

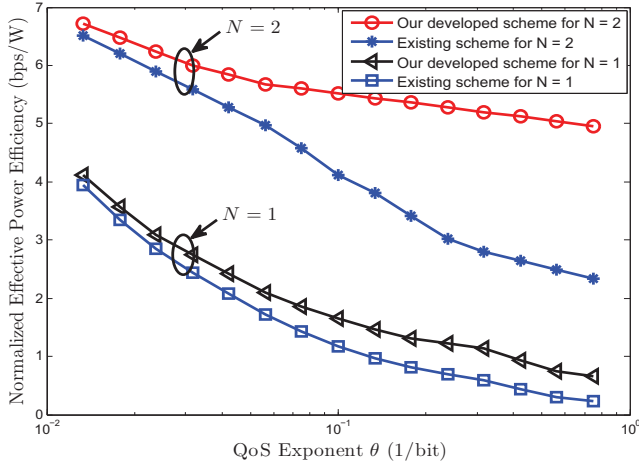


Fig. 8. The comparison between our developed QoS-driven green power allocation schemes and existing schemes.

ignored (corresponding to the plot with legend “Power allocation scheme given by Lemma 1” in Fig. 6 and the plot with legend “Only average power constraint in Fig. 7”). Thus, as a result, as shown in Figs. 6 and 7, our developed QoS-driven green power allocation schemes yield the best EPE as compared with the QoS-driven power allocation schemes which only take into account the average power constraints. For the power allocation schemes without taking into account the delay-bounded QoS provisioning, the maximum EPE can only be achieved at the very loose or very stringent delay-bounded QoS requirements because these schemes are in nature designed for the fixed delay-bounded QoS requirements (corresponding to the plots with legends “Despicking water-filling scheme” and “Despicking channel inversion scheme” in Fig. 6, and the plots with legends “DWF scheme when  $N = 2$ ” and “DCI scheme when  $N = 2$ ” in Fig. 7).

Figure 8 compares our developed QoS-driven green power allocation schemes with the existing related research work [18], where the authors developed the power allocation schemes to maximize capacity under average and peak power constraints. As illustrated in Fig. 8, we can observe that our developed QoS-driven green power allocation schemes achieve larger EPE as compared with that developed in [18]. This is because our developed optimal schemes are adaptive to diverse delay-bounded QoS constraints, thus achieving the maximum EPE under any delay-bounded QoS constraint. For both SISO and MIMO scenarios, the EPE improvement (Here, the EPE improvement is the obtained EPE using our developed QoS-driven green power allocation schemes minus the obtained EPE using the schemes developed in [18]) under stringent delay-bounded QoS requirements (for example,  $\theta$  is near to 1 in Fig. 8) is relatively larger than the EPE improvement under loose delay-bounded QoS requirements (for example,  $\theta$  is near to 0.01 in Fig. 8). This is because the schemes developed in [18] is designed for the very loose delay-bound QoS constraints. The EPE improvement in MIMO scenario is much larger than the EPE improvement in SISO scenario. This is because our developed optimal schemes are adaptive to multiple antennas scenarios. When QoS exponent is small,

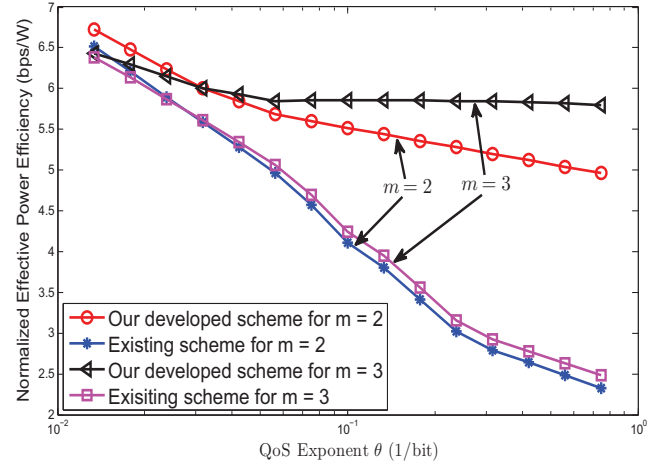


Fig. 9. The effect of Nakagami fading parameter  $m$  on our developed QoS-driven green power allocation schemes and the other existing schemes.

representing that the delay-bounded QoS power allocation scheme is very loose, the schemes developed in [18] can achieve the similar EPE as compared with our developed schemes. However, the EPE using our developed schemes always outperforms the EPE using the schemes developed in [18].

Figure 9 shows the effect of Nakagami fading parameter  $m$  on our developed QoS-driven green power allocation schemes and the other existing schemes developed in reference [18]. For the scenario corresponding to loose delay-bounded QoS constraint, the EPE decreases as  $m$  increases. For the scenario corresponding to stringent delay-bounded QoS constraint, the EPE increases as the Nakagami fading parameter  $m$  increases. Also, as  $m$  increases from 2 to 3 under the stringent delay-bounded QoS constraint, our developed QoS-driven green power allocation schemes can significantly increase the EPE while the other existing schemes can only yield very slight improvement on the EPE.

Figure 10 shows the EPE of our QoS-driven green power allocation scheme, the DWF scheme, the DCI scheme for the MIMO-channel, and the EPE of the SISO-channel when only considering the peak power constraint. As illustrated in Fig. 10, when  $\theta \rightarrow 0$ , the QoS-driven green power allocation scheme for  $N = 2$  can achieve a 3 dB EPE gain as compared with the QoS-driven green power allocation scheme for  $N = 1$ . When  $\theta \rightarrow \infty$ , the QoS-driven green power allocation scheme for  $N = 2$  can achieve much larger EPE gain than the QoS-driven green power allocation scheme for  $N = 1$ .

## VI. CONCLUSIONS

We tackled the problem on how to maximize the energy efficiency while guaranteeing the QoS of 5G wireless networks. We proposed the EPE framework and developed the QoS-driven green power allocation schemes to maximize the EPE of SISO-channel and MIMO-channel based 5G wireless network, respectively, under joint average and peak power constraints. We also derived the conditions that our developed QoS-driven green power allocation schemes are dominated by

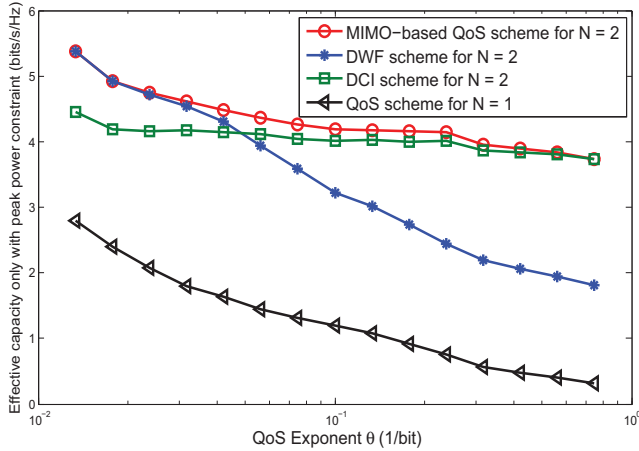


Fig. 10. The EPE of our MIMO-based QoS-driven power allocation scheme, the despiking water-filling scheme, the despiking channel inversion scheme for MIMO-channel, and the QoS-driven power allocation scheme for SISO-channel when only considering the peak power constraint.

joint the average and the peak power constraints, only the peak power constraint, and only the average power constraint for the SISO-channel and the MIMO-channel based wireless network, respectively. The obtained numerical results show that our QoS-driven green power allocation schemes can maximize EPE, thus enabling the effective implementation of green and QoS-guaranteed 5G mobile wireless networks. The results obtained in our proposed energy-efficient (green) homogeneous statistical delay-bounded QoS provisioning can be used as the benchmarks to compare with those to be obtained for the energy-efficient (green) heterogeneous statistical delay-bounded QoS provisioning, which will be addressed in our next paper of the future work.

#### APPENDIX A PROOF OF THEOREM 1

*Proof:* If the optimal power allocation scheme is determined by only the average power constraint, the following equation need to be satisfied for any given  $\beta$ :

$$f_a(\gamma) \triangleq \frac{\bar{P}}{\gamma_t^{\frac{1}{\beta+1}} \gamma^{\frac{\beta}{\beta+1}}} - \frac{\bar{P}}{\gamma} \leq P_{\text{peak}}, \quad \forall \beta \in (0, \infty). \quad (53)$$

To obtain the maximum value of  $f_a(\gamma)$ , we divide  $f_a(\gamma)$  into three parts as follows:

**Part I** ( $\theta < \theta_w(\bar{P}, P_{\text{peak}})$ ): The very loose delay-QoS constraint (water-filling-like) mode.

**Part II** ( $\theta > \theta_c(\bar{P}, P_{\text{peak}})$ ): The very stringent delay-QoS constraint (channel-inversion-like) mode.

**Part III** ( $\theta_w(\bar{P}, P_{\text{peak}}) \leq \theta \leq \theta_c(\bar{P}, P_{\text{peak}})$ ): The not very loose and not very stringent delay-QoS constraint mode.

For very loose QoS constraint ( $\theta \rightarrow 0$ ),  $f_a(\gamma)$  converts to

$$f_a(\gamma) = \frac{\bar{P}}{\gamma_t} - \frac{\bar{P}}{\gamma}. \quad (54)$$

When  $\theta \rightarrow 0$ , the maximum value of  $f_a(\gamma)$  is obtained at  $\gamma \rightarrow \infty$ . Thus, for **Part I**, the maximum power is allocated

at  $\gamma \rightarrow \infty$ . In this part, if  $P_{\text{peak}} \geq (\bar{P}/\gamma_t)$ , the peak power constraint is always satisfied.

For very stringent QoS constraint ( $\theta \rightarrow \infty$ ),  $f_a(\gamma)$  turns to

$$f_a(\gamma) = \frac{\sigma}{\gamma}, \quad (55)$$

where  $\sigma = \lim_{\theta \rightarrow \infty} \bar{P} \gamma_t^{-\frac{1}{\beta+1}} - \bar{P}$ . When  $\theta \rightarrow \infty$ ,  $f_a(\gamma)$  decreases as  $\gamma$  increases and the maximum value of  $f_a(\gamma)$  is obtained at  $\gamma \rightarrow \gamma_t^+$ , where  $x \rightarrow x_0^+$  denotes that  $x$  approaches  $x_0$  from the right. Thus, for **Part II**, the maximum power is allocated at  $\gamma \rightarrow \gamma_t^+$ . In this part, if  $P_{\text{peak}} \geq \lim_{\gamma \rightarrow \gamma_t^+} (\sigma/\gamma)$ , the peak power constraint is always satisfied.

For **Part III**, because  $f_a(\gamma)$  is a concave function of  $\gamma$  with a fixed  $\beta$ , the maximum value of  $f_a(\gamma)$  is obtained at the point where the derivative is equal to zero. Taking the derivative of  $f_a(\gamma)$  with respect to  $\gamma$  and setting the result to zero, we have

$$\frac{\partial f_a(\gamma)}{\partial \gamma} = \frac{\bar{P}}{\gamma_t^{\frac{1}{\beta+1}}} \left( -\frac{\beta}{\beta+1} \right) \frac{1}{\gamma^{\frac{2\beta+3}{\beta+1}}} + \frac{\bar{P}}{\gamma^2} = 0. \quad (56)$$

Because  $\gamma > 0$  and  $\bar{P} > 0$ , solving Eq. (56) we can derive

$$\gamma = \gamma_t \left( \frac{\beta+1}{\beta} \right)^{\beta+1}. \quad (57)$$

Substituting Eq. (57) into Eq. (53), we can obtain that for this part if

$$P_{\text{peak}} \geq \frac{\bar{P} \beta^\beta}{\gamma_t (\beta+1)^{\beta+1}} \quad (58)$$

holds, the peak power constraint is always satisfied. Therefore, to ensure Eq. (53) to be always satisfied for any given  $\beta$ ,  $P_{\text{peak}}$  need to satisfy the following condition:

$$P_{\text{peak}} \geq \max_{\gamma} \left\{ \left( \frac{\bar{P}}{\gamma_t} \right), \lim_{\gamma \rightarrow \gamma_t^+} \left( \frac{\sigma}{\gamma} \right), \frac{\bar{P} \beta^\beta}{\gamma_t (\beta+1)^{\beta+1}} \right\} \\ \stackrel{(a)}{=} \max_{\gamma} \left\{ \left( \frac{\bar{P}}{\gamma_t} \right), \lim_{\gamma \rightarrow \gamma_t^+} \left( \frac{\sigma}{\gamma} \right) \right\} \quad (59)$$

where  $\max\{c_1, c_2, c_3\}$  denotes the maximum of  $c_1$ ,  $c_2$ , and  $c_3$ ,  $\max\{d_1, d_2\}$  represents the maximum of  $d_1$  and  $d_2$ . Because for any  $0 < \beta < \infty$ , we have  $0 < [(\bar{P} \beta^\beta) / (\gamma_t (\beta+1)^{\beta+1})] < (\bar{P}/\gamma_t)$ , and thus, (a) in Eq. (59) holds. On the other hand, because of (a) in Eq. (59), we have:

$$\max \left\{ \left( \frac{\bar{P}}{\gamma_t} \right), \lim_{\gamma \rightarrow \gamma_t^+} \left( \frac{\sigma}{\gamma} \right) \right\} = \max_{\gamma} \{f_a(\gamma)\} = g(\bar{P}) \quad (60)$$

which holds for **Part I**, **Part II**, and **Part III**. Thus, we obtain:

$$g(\bar{P}) = \max \left\{ \left( \frac{\bar{P}}{\gamma_t} \right), \lim_{\gamma \rightarrow \gamma_t^+} \left( \frac{\sigma}{\gamma} \right) \right\}, \quad (61)$$

which is Eq. (12), completing the proof. ■

APPENDIX B  
PROOF OF THEOREM 2

*Proof:* The Lagrangian function for problem **P2** is given by

$$J_1 = \mathbb{E}_\gamma [(1 + P(\boldsymbol{\nu})\gamma)^{-\beta}] + \rho_1 \{ \mathbb{E}_\gamma [P(\boldsymbol{\nu})] - \bar{P} \} + \rho_2 [P(\boldsymbol{\nu}) - P_{\text{peak}}] \quad (62)$$

where  $\rho_1$  and  $\rho_2$  are the Lagrangian multipliers corresponding to the average power constraint and the peak power constraint, respectively. The Karush-Kuhn-Tucker (KKT) conditions for problem **P2** can be written as [30]

$$\begin{cases} -\beta\gamma [1 + P(\boldsymbol{\nu})\gamma]^{-\beta-1} p_\Gamma(\gamma) + \rho_1 p_\Gamma(\gamma) + \rho_2 = 0; \\ \rho_1 \{ \mathbb{E}_\gamma [P(\boldsymbol{\nu})] - \bar{P} \} = 0; \\ \rho_1 \geq 0; \\ \rho_2 [P(\boldsymbol{\nu}) - P_{\text{peak}}] = 0; \\ \rho_2 \geq 0; \end{cases} \quad (63)$$

Based on the above conditions, we can obtain the optimal power allocation scheme as follows:

$$P(\boldsymbol{\nu}) = \frac{\bar{P}}{\gamma_0^{\frac{1}{\beta+1}} \gamma^{\frac{\beta}{\beta+1}}} - \frac{\bar{P}}{\gamma}, \quad (64)$$

where  $\gamma_0 = \rho_1/\beta$ . Then, because Eq. (64) need to satisfy  $0 \leq P(\boldsymbol{\nu}) \leq P_{\text{peak}}$ , we can obtain Eq. (16), which completes the proof. ■

APPENDIX C  
PROOF OF THEOREM 3

*Proof:* To solve problem **P3**, we formulate the Lagrangian function as follows:

$$\begin{aligned} \mathcal{J}_m = & \underbrace{\mathbb{E}_{\lambda_1} \cdots \mathbb{E}_{\lambda_N}}_{N\text{-fold}} \left\{ \prod_{n=1}^N [1 + P_n(\tilde{\boldsymbol{\nu}})\lambda_n^2]^{-\beta} \right\} \\ & + \kappa_0 \left\{ \sum_{n=1}^N \left[ \underbrace{\mathbb{E}_{\lambda_1} \cdots \mathbb{E}_{\lambda_N}}_{N\text{-fold}} (P_n(\tilde{\boldsymbol{\nu}})) \right] - \bar{P} \right\} \\ & - \sum_{n=1}^N \kappa_n P_n(\tilde{\boldsymbol{\nu}}) + \mu \left( \sum_{n=1}^N P_n(\tilde{\boldsymbol{\nu}}) - P_{\text{peak}} \right) \end{aligned} \quad (65)$$

where  $\kappa_1, \kappa_2, \dots, \kappa_N$  denote the Lagrangian multipliers corresponding to the constraints that force the power allocated to each antenna to be positive,  $\mu$  represents the Lagrangian multiplier corresponding to the peak power constraint, and  $\kappa_0$  is the Lagrangian multiplier corresponding to the average power constraint.

The KKT conditions can be given by [30]

$$\begin{cases} -\beta\lambda_n^2 [1 + P_n(\tilde{\boldsymbol{\nu}})\lambda_n^2]^{-\beta-1} f(\boldsymbol{\lambda}) \prod_{i \in N, i \neq n} [1 + P_i(\tilde{\boldsymbol{\nu}})\lambda_i^2]^{-\beta} \\ \quad + \kappa_0 f(\boldsymbol{\lambda}) - \kappa_n + \mu = 0, \quad n = 1, 2, \dots, N; \quad (66a) \\ \kappa_n P_n(\tilde{\boldsymbol{\nu}}) = 0, \quad n = 1, 2, \dots, N; \quad (66b) \\ \kappa_n \geq 0, \quad n = 1, 2, \dots, N; \quad (66c) \\ P_n(\tilde{\boldsymbol{\nu}}) \geq 0, \quad n = 1, 2, \dots, N; \quad (66d) \\ \mu \geq 0; \quad (66e) \\ \mu \left[ \sum_{n=1}^N P_n(\tilde{\boldsymbol{\nu}}) - P_{\text{peak}} \right] = 0; \quad (66f) \\ \sum_{n=1}^N \mathbb{E}_{\boldsymbol{\lambda}} \{ P_n(\tilde{\boldsymbol{\nu}}) \} = \bar{P}, \quad (66g) \end{cases}$$

where Eq. (66g) is derived because the maximum effective capacity is obtained when the average power constraint is satisfied with equality. We consider two cases: **Case III(A)** and **Case III(B)** as follows.

**Case III(A):**  $\sum_{n=1}^N P_n(\tilde{\boldsymbol{\nu}}) < P_{\text{peak}}$ . Note that all the power is assigned to the channels which belong to  $\mathcal{N}_1$ . In [11], a recursive algorithm was proposed to identify the channels to which non-zero power is allocated based on the instantaneous CSI. Given that  $\sum_{n=1}^N P_n(\tilde{\boldsymbol{\nu}}) < P_{\text{peak}}$  and the complementary slackness condition [30], we have  $\kappa_n = 0$  ( $n = 1, 2, \dots, N_1$ ) and  $\mu = 0$ . Therefore, in this case, Eq. (66a) reduces to

$$-\beta\lambda_n^2 [1 + P_n(\tilde{\boldsymbol{\nu}})\lambda_n^2]^{-1} \cdot \prod_{i \in N_1} [1 + P_i(\tilde{\boldsymbol{\nu}})\lambda_i^2]^{-\beta} + \kappa_0 = 0, \quad n = 1, 2, \dots, N_1. \quad (67)$$

Denoting  $\alpha_n = 1 + P_n(\tilde{\boldsymbol{\nu}})\lambda_n^2$  and  $A = \prod_{i \in N_1} \alpha_i^{-\beta}$ , from Eq. (67), we have

$$\alpha_n = \frac{\beta\lambda_n^2}{\kappa_0} \prod_{i \in N_1} \alpha_i^{-\beta}. \quad (68)$$

Thus, we can obtain

$$A = \prod_{i \in N_1} \left( \frac{\beta\lambda_i^2}{\kappa_0} A \right)^{-\beta} = A^{-N_1\beta} \prod_{i \in N_1} \left( \frac{\beta\lambda_i^2}{\kappa_0} \right)^{-\beta}. \quad (69)$$

Solving Eq. (69), we can derive

$$A = \prod_{i \in N_1} \left( \frac{\beta\lambda_i^2}{\kappa_0} \right)^{-\frac{\beta}{1+N_1\beta}}. \quad (70)$$

Therefore, the closed-form solution of  $\alpha_n$  is given by

$$\alpha_n = \frac{\beta\lambda_n^2}{\kappa_0} A = \left( \frac{\beta}{\kappa_0} \right)^{\frac{1}{1+N_1\beta}} \lambda_n^2 \prod_{i \in N_1} \lambda_i^{-\frac{2\beta}{1+N_1\beta}}. \quad (71)$$

The power allocation policy for  $n \in N_1$  can be obtained as follows:

$$P_n(\tilde{\boldsymbol{\nu}}) = \begin{cases} \frac{\bar{P}}{\left( \frac{\kappa_0}{\beta} \right)^{\frac{1}{1+N_1\beta}} \prod_{i \in N_1} \lambda_i^{\frac{2\beta}{1+N_1\beta}}} - \frac{\bar{P}}{\lambda_n^2}, & \text{if } n \in N_1; \\ 0, & \text{if } n \in N_0. \end{cases} \quad (72)$$

**Case III(B):**  $\sum_{n=1}^{N_1} P_n(\tilde{\nu}) = P_{\text{peak}}$ . In this case, using the complementary slackness condition [30], Eq. (66a) can be reduced to

$$\left( -\beta \lambda_n^2 [1 + P_n(\tilde{\nu}) \lambda_n^2]^{-1} \prod_{i \in N_1} [1 + P_i(\tilde{\nu}) \lambda_i^2]^{-\beta} + \kappa_0 \right) \cdot f(\lambda) + \mu = 0, \quad n = 1, 2, \dots, N_1. \quad (73)$$

Solving Eq. (73), we can obtain

$$P_n(\tilde{\nu}) = \begin{cases} \frac{\bar{P}}{\lambda_n^2} - \frac{\frac{1}{1+N_1\beta}}{\left(\frac{\kappa_0}{\beta} + \frac{\mu}{\beta f(\lambda)}\right) \prod_{i \in N_1} \lambda_i^{\frac{2\beta}{1+N_1\beta}}}, & \text{if } n \in N_1; \\ 0, & \text{if } n \in N_0. \end{cases} \quad (74)$$

Thus, Theorem 3 follows. ■

### REFERENCES

[1] K. Davaslioglu and E. Ayanoglu, "Quantifying potential energy efficiency gain in green cellular wireless networks," *IEEE Communications Surveys Tutorials*, vol. 16, no. 4, pp. 2065–2091, Fourthquarter 2014.

[2] C. Han, T. Harrold, S. Armour, I. Krikidis, S. Videv, P. M. Grant, H. Haas, J. S. Thompson, I. Ku, C.-X. Wang, T. A. Le, M. R. Nakhai, J. Zhang, and L. Hanzo, "Green radio: radio techniques to enable energy-efficient wireless networks," *IEEE Communications Magazine*, vol. 49, no. 6, pp. 46–54, June 2011.

[3] C.-X. Wang, F. Haider, X. Gao, X.-H. You, Y. Yang, D. Yuan, H. Aggoune, H. Haas, S. Fletcher, and E. Hepsaydir, "Cellular architecture and key technologies for 5G wireless communication networks," *IEEE Communications Magazine*, vol. 52, no. 2, pp. 122–130, Feb. 2014.

[4] Y. Chen, S. Zhang, S. Xu, and G. Y. Li, "Fundamental trade-offs on green wireless networks," *IEEE Communications Magazine*, vol. 49, no. 6, pp. 30–37, June 2011.

[5] W. Cheng, X. Zhang, H. Zhang, and Q. Wang, "On-demand based wireless resources trading for green communications," in *IEEE INFOCOM 2011*, Apr. 2011, pp. 283–288.

[6] G. Caire, G. Taricco, and E. Biglieri, "Optimum power control over fading channels," *IEEE Transactions on Information Theory*, vol. 45, no. 5, pp. 1468–1489, July 1999.

[7] W. Cheng, X. Zhang, and H. Zhang, "QoS driven power allocation over full-duplex wireless links," in *IEEE International Conference on Communications (ICC)*, June 2012, pp. 5286–5290.

[8] D. Wu and R. Negi, "Effective capacity: a wireless link model for support of quality of service," *IEEE Transactions on Wireless Communications*, vol. 2, no. 4, pp. 630–643, July 2003.

[9] X. Zhang and J. Tang, "Power-delay tradeoff over wireless networks," *IEEE Transactions on Communications*, vol. 61, no. 9, pp. 3673–3684, September 2013.

[10] J. Tang and X. Zhang, "Quality-of-service driven power and rate adaptation over wireless links," *IEEE Transactions on Wireless Communications*, vol. 6, no. 8, pp. 3058–3068, Aug. 2007.

[11] J. Tang and X. Zhang, "Quality-of-service driven power and rate adaptation for multichannel communications over wireless links," *IEEE Transactions on Wireless Communications*, vol. 6, no. 12, pp. 4349–4360, Dec. 2007.

[12] X. Zhang and Q. Du, "Cross-layer modeling for QoS-driven multimedia multicast/broadcast over fading channels in mobile wireless networks," *IEEE Communications Magazine*, vol. 45, no. 8, pp. 62–70, Aug. 2007.

[13] Q. Du and X. Zhang, "Statistical QoS provisionings for wireless unicast/multicast of multi-layer video streams," *IEEE Journal on Selected Areas in Communications*, vol. 28, no. 3, pp. 420–433, Apr. 2010.

[14] S. Ren and K. B. Letaief, "Maximizing the effective capacity for wireless cooperative relay networks with QoS guarantees," *IEEE Transactions on Communications*, vol. 57, no. 7, pp. 2148–2159, July 2009.

[15] R. Q. Hu and Y. Qian, "An energy efficient and spectrum efficient wireless heterogeneous network framework for 5G systems," *IEEE Communications Magazine*, vol. 52, no. 5, pp. 94–101, May 2014.

[16] Y. Wu, J. Wang, L. Qian, and R. Schober, "Optimal power control for energy efficient D2D communication and its distributed implementation," *IEEE Communications Letters*, vol. 19, no. 5, pp. 815–818, May 2015.

[17] G. Liu, F. R. Yu, H. Ji, and V. C. M. Leung, "Energy-efficient resource allocation in cellular networks with shared full-duplex relaying," *IEEE Transactions on Vehicular Technology*, vol. 64, no. 8, pp. 3711–3724, Aug. 2015.

[18] A. Zappone, L. Sanguinetti, G. Bacci, E. Jorswieck, and M. Debbah, "Energy-efficient power control: A look at 5G wireless technologies," to appear in *IEEE Transactions on Signal Processing*, 2015.

[19] C. X. Mavroumoustakis, G. Mastorakis, A. Bourdena, E. Pallis, G. Kormentzas, and C. D. Dimitriou, "Joint energy and delay-aware scheme for 5G mobile cognitive radio networks," in *IEEE GLOBECOM 2014*, Dec. 2014, pp. 2624–2630.

[20] L. Musavian and T. Le-Ngoc, "Energy-efficient power allocation over Nakagami- $m$  fading channels under delay-outage constraints," *IEEE Transactions on Wireless Communications*, vol. 13, no. 8, pp. 4081–4091, Aug. 2014.

[21] M. Sinaie, A. Zappone, E. Jorswieck, and P. Azmi, "A novel power consumption model for effective energy efficiency in wireless networks," *IEEE Wireless Communications Letters*, vol. PP, no. 99, pp. 1–1, 2015.

[22] X. Zhang, W. Cheng, and H. Zhang, "Heterogeneous statistical QoS provisioning over 5G mobile wireless networks," *IEEE Network*, vol. 28, no. 6, pp. 46–53, Nov. 2014.

[23] C.-S. Chang, "Stability, queue length, and delay of deterministic and stochastic queueing networks," *IEEE Transactions on Automatic Control*, vol. 39, no. 5, pp. 913–931, May 1994.

[24] X. Zhang, J. Tang, H. H. Chen, S. Ci, and M. Guizani, "Cross-layer-based modeling for quality of service guarantees in mobile wireless networks," *IEEE Communications Magazine*, vol. 44, no. 1, pp. 100–106, 2006.

[25] A. J. Goldsmith and S.-G. Chua, "Variable-rate variable-power MQAM for fading channels," *IEEE Transactions on Communications*, vol. 45, no. 10, pp. 1218–1230, Oct. 1997.

[26] E. Telatar, "Capacity of multi-antenna Gaussian channels," *Eur. Trans. Telecomm. ETT*, vol. 10, no. 6, pp. 585–596, Nov. 1999.

[27] M. Nakagami, "The  $m$ -distribution – a general formula for intensity distribution of rapid fading," *Statistical Methods in Radio Wave Propagation*, pp. 3–36, 1960.

[28] G. K. Karagiannidis, D. A. Zogas, and S. A. Kotsopoulos, "An efficient approach to multivariate Nakagami- $m$  distribution using Green's matrix approximation," *IEEE Transactions on Wireless Communications*, vol. 2, no. 5, pp. 883–889, Sep. 2003.

[29] R. Nabben, "On Green's matrices of trees," *SIAM J. Matrix Anal. Appl.*, vol. 4, pp. 1014–1026, 2000.

[30] S. Boyd and L. Vandenberghe, *Convex Optimization*, Cambridge University Press, 2004.



**Wenchi Cheng** (M'14) received the B.S. degree and Ph.D. degree in Telecommunication Engineering from Xidian University, China, in 2008 and 2014, respectively. He joined Department of Telecommunication Engineering, Xidian University, in 2013, as an Assistant Professor. He worked as a visiting Ph.D. student under the supervision of Professor Xi Zhang at Networking and Information Systems Laboratory, Department of Electrical and Computer Engineering, Texas A&M University, College Station, Texas, U.S.A., from 2010 to 2011.

His research interests focus on 5G wireless networks, wireless full-duplex transmission, statistical QoS provisioning, cognitive radio techniques, and energy efficient wireless networks. He has published multiple papers in *IEEE JOURNAL ON SELECTED AREAS IN COMMUNICATIONS*, *IEEE WIRELESS COMMUNICATIONS MAGAZINE*, *IEEE NETWORK MAGAZINE*, *IEEE TRANS.*, *IEEE INFOCOM*, *IEEE GLOBECOM*, *IEEE ICC*, etc. He is serving as the Technical Program Committee (TPC) member for *IEEE ICC 2016*, *IEEE GLOBECOM 2016*, and *IEEE INFOCOM 2016*.



**Xi Zhang** (S'89-SM'98-F'16) received the B.S. and M.S. degrees from Xidian University, Xi'an, China, the M.S. degree from Lehigh University, Bethlehem, PA, all in electrical engineering and computer science, and the Ph.D. degree in electrical engineering and computer science (Electrical Engineering-Systems) from The University of Michigan, Ann Arbor, MI, USA.

He is currently a Full Professor and the Founding Director of the Networking and Information Systems Laboratory, Department of Electrical and Computer Engineering, Texas A&M University, College Station. He is a Fellow of the IEEE for contributions to quality of service (QoS) in mobile wireless networks. He was with the Networks and Distributed Systems Research Department, AT&T Bell Laboratories, Murray Hill, New Jersey, and AT&T Laboratories Research, Florham Park, New Jersey, in 1997. He was a research fellow with the School of Electrical Engineering, University of Technology, Sydney, Australia, and the Department of Electrical and Computer Engineering, James Cook University, Australia. He has published more than 300 research papers on wireless networks and communications systems, network protocol design and modeling, statistical communications, random signal processing, information theory, and control theory and systems. He received the U.S. National Science Foundation CAREER Award in 2004 for his research in the areas of mobile wireless and multicast networking and systems. He is an IEEE Distinguished Lecturer of both IEEE Communications Society and IEEE Vehicular Technology Society. He received Best Paper Awards at IEEE GLOBECOM 2014, IEEE GLOBECOM 2009, IEEE GLOBECOM 2007, and IEEE WCNC 2010, respectively. One of his IEEE Journal on Selected Areas in Communications papers has been listed as the IEEE Best Readings (receiving the top citation rate) Paper on Wireless Cognitive Radio Networks and Statistical QoS Provisioning over Mobile Wireless Networking. He also received a TEES Select Young Faculty Award for Excellence in Research Performance from the Dwight Look College of Engineering at Texas A&M University, College Station, in 2006.

Prof. Zhang is serving or has served as an Editor for IEEE TRANSACTIONS ON COMMUNICATIONS, IEEE TRANSACTIONS ON WIRELESS COMMUNICATIONS, and IEEE TRANSACTIONS ON VEHICULAR TECHNOLOGY, twice as a Guest Editor for IEEE JOURNAL ON SELECTED AREAS IN COMMUNICATIONS for two special issues on Broadband Wireless Communications for High Speed Vehicles and Wireless Video Transmissions, an Associate Editor for IEEE COMMUNICATIONS LETTERS, twice as the Lead Guest Editor for *IEEE Communications Magazine* for two special issues on "Advances in Cooperative Wireless Networking" and "Underwater Wireless Communications and Networks: Theory and Applications", and a Guest Editor for *IEEE Wireless Communications Magazine* for special issue on "Next Generation CDMA vs. OFDMA for 4G Wireless Applications", an Editor for Wileys JOURNAL ON WIRELESS COMMUNICATIONS AND MOBILE COMPUTING, JOURNAL OF COMPUTER SYSTEMS, NETWORKING, AND COMMUNICATIONS, and Wileys JOURNAL ON SECURITY AND COMMUNICATIONS NETWORKS, and an Area Editor for Elseviers JOURNAL ON COMPUTER COMMUNICATIONS, among many others. He is serving or has served as the TPC Chair for IEEE GLOBECOM 2011, TPC Vice-Chair IEEE INFOCOM 2010, TPC Area Chair for IEEE INFOCOM 2012, Panel/Demo/Poster Chair for ACM MobiCom 2011, General Vice-Chair for IEEE WCNC 2013, and TPC/General Chair for numerous other IEEE/ACM conferences, symposia, and workshops.



**Hailin Zhang** (M'98) received B.S. and M.S. degrees from Northwestern Polytechnic University, Xi'an, China, in 1985 and 1988 respectively, and the Ph.D. from Xidian University, Xi'an, China, in 1991. In 1991, he joined School of Telecommunications Engineering, Xidian University, where he is a senior Professor and the Dean of this school. He is also currently the Director of Key Laboratory in Wireless Communications Sponsored by China Ministry of Information Technology, a key member of State Key Laboratory of Integrated Services Networks, one of

the state government specially compensated scientists and engineers, a field leader in Telecommunications and Information Systems in Xidian University, an Associate Director for National 111 Project. Dr. Zhang's current research interests include key transmission technologies and standards on broadband wireless communications for 5G wireless access systems. He has published more than 100 papers in journals and conferences.